Smart Knives:

Controlled cutting schemes to enable advanced endoscopic surgery

Towards dye-mediated laser ablation

Ifung Lu PhD candidate
Supervised by **Tim N. Mills** PhD, **Sandy Mosse** PhD

Research goal: To invent new controlled cutting schemes to enable advanced endoscopic surgery.

Questions:

1. Why? — **Why** should we do it?
   Invent new cutting tools?
2. What? — **What** should we do?
   Is white space is available?
3. How? — **How** do we do it?
   Deconstructing Dissection
4. How? — **How** do we **really** do it?
   Dye-mediated laser ablation

Why should we do it?

Invent new cutting tools?

The historical trend in medicine and surgery has been to treat patients using progressively less invasive methods.

Cuschieri & Berci (1991) → **Rao & Reddy (2006)**

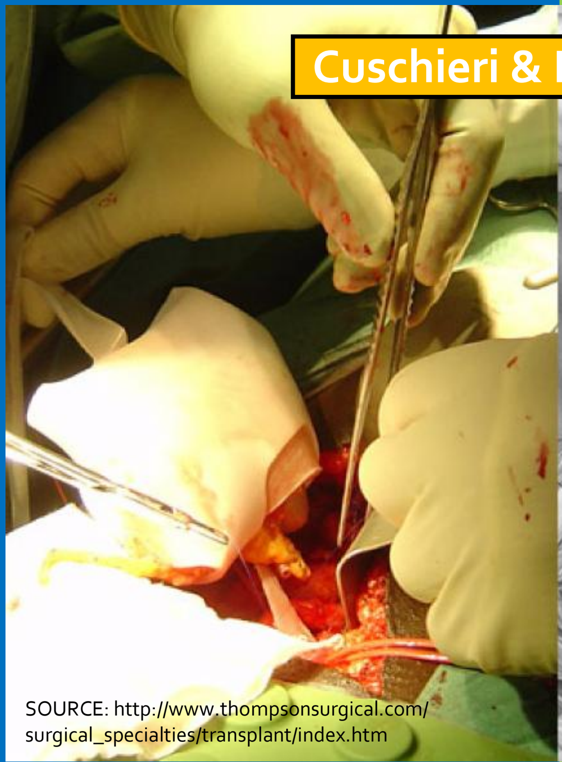

SOURCE: http://www.thompsonsurgical.com/surgical_specialties/transplant/index.htm

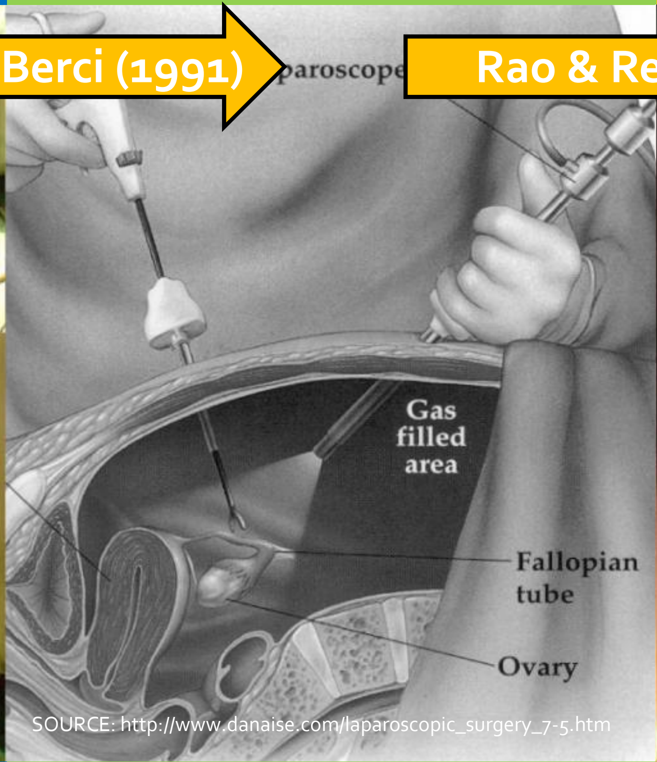

SOURCE: http://www.danaise.com/laparoscopic_surgery_7-5.htm

Open Surgery
One large external incision
Hands, tools
Excellent control

Laparoscopic Surgery
Multiple small external incisions
Laparoscopic instruments
Restricted control

Endoscopic Surgery
One small internal incision
Endoscopic instruments
Poor control

Natural orifice transluminal endoscopic surgery (NOTES) may be the next evolution of minimally invasive surgery.

- NOTES may be useful for treatment of the **morbidly obese** or **palliative relief** for the deathly ill. (Hocheberger & Lamadé 2005)
- NOTES might **improve access** … for some bariatric procedures. (Swain 2007)
- *"There are three steps in the revelation of any truth: In the first, it is ridiculed; in the second, resisted; in the third, it is considered self-evident."* (Valdivieso et al. 2007)

New cutting tools may be required to enable advanced endoscopic surgery, including NOTES.

- NOSCAR white paper reviewed **barriers to NOTES**. (Hawes et al. 2006)
- Creation of an **endoscopic toolset** and new "**deconstructed endoscopes**". (Swain & Kochman 2007)
- **Colloboration** between clinicians and technicians necesary to develop new instruments for transgastric surgery. (Swanstrom et al. 2007)
- Need for **tissue retraction** and **instrument triangulation**. (Nakao 2007)
- TEM, rendezvous / hybrid approaches also feasible. (Denk, Swanström & Whiteford 2008, Romanelli & Earle 2009)
- New tech – grasping ESD **scissors**, cap **suturing system**, bipolar **haemostasis forceps**. (Akahoshi et al. 2008; Moran, Gostout & Bingener 2009; Park et al. 2010)

What has been done?

Is white space is available?

Existing Tools

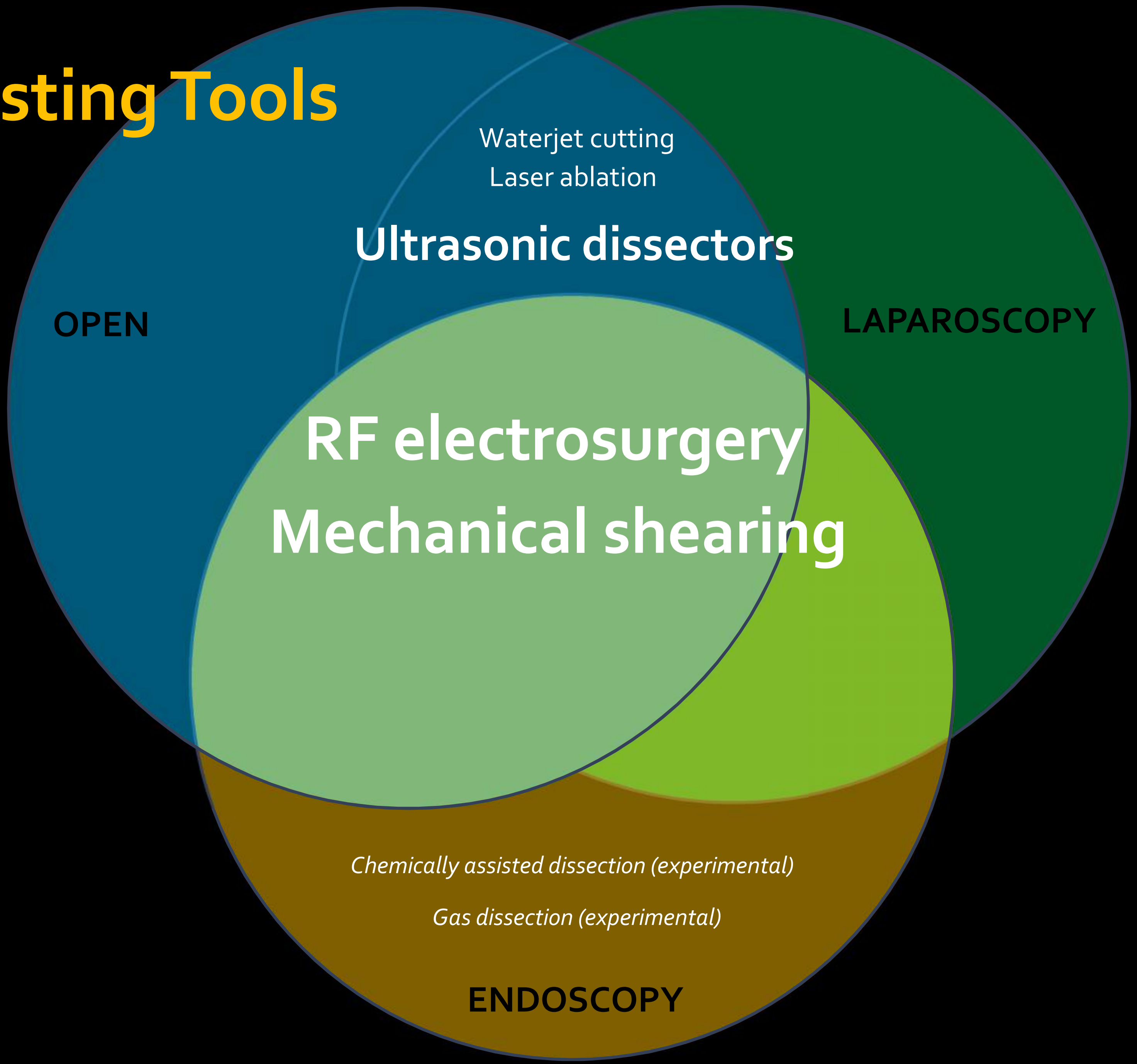

Existing Control

Sensitizing with chemicals

Feedback control

Articulation

(Reproduced from Richards et. al.)

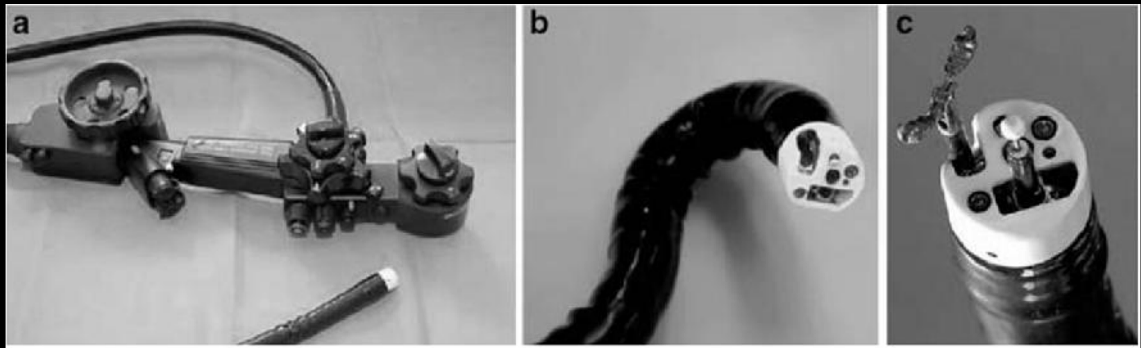

(Reproduced from Reavis and Melvin.)

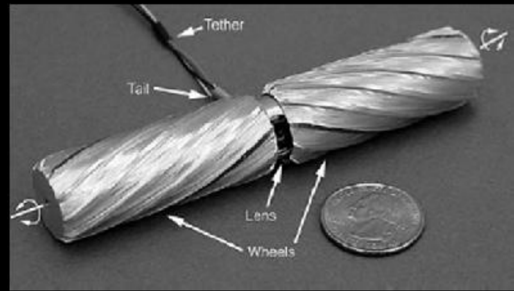

(Reproduced from Rentschler and Oleynikov.)

(Personal photographs)

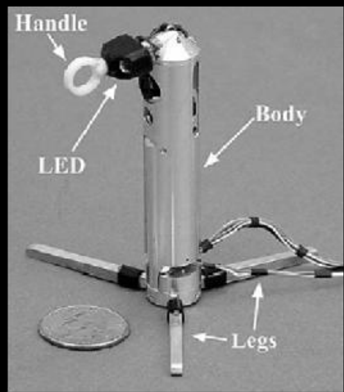

(Reproduced from Rentschler and Oleynikov.)

(Reproduced from Ishikawa et. al)

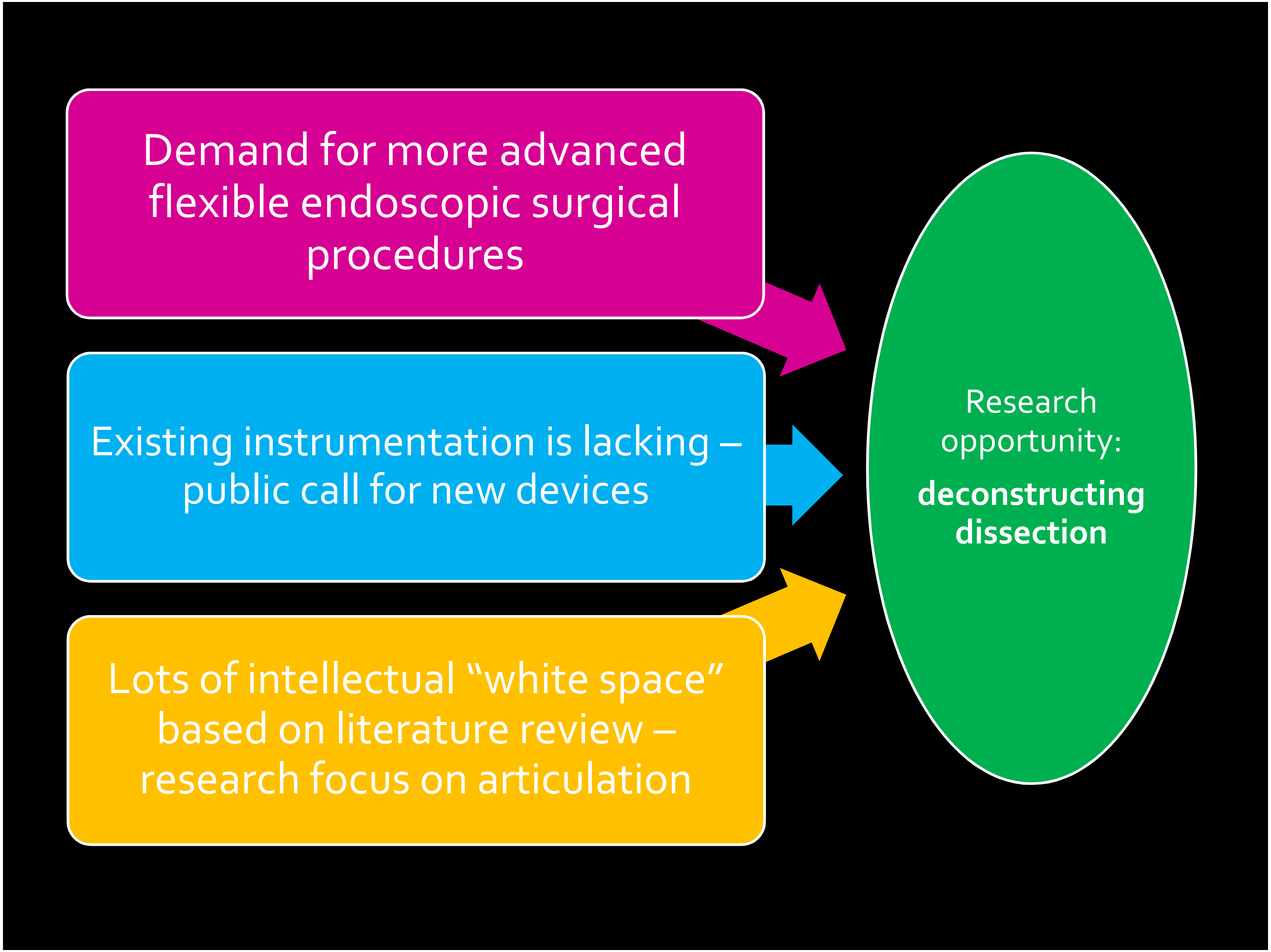
Demand for more advanced flexible endoscopic surgical procedures
Existing instrumentation is lacking – public call for new devices
Lots of intellectual "white space" based on literature review – research focus on articulation
Research opportunity:
deconstructing dissection

How can we improve control?

Deconstructing Dissection

Tissue dissection

==

Target ~~and~~ *then* Cut

Deconstructing Dissection —
Target then Cut (sequential tasks, not simultaneous)

Deconstructing Dissection

Local tissue tensioning

Blunt dissection by
gas-evolving chemical reaction

Selective tissue stiffening

Electrically conductive
or insulating masks

**Dye-mediated
laser ablation**

Acoustic fingerprinting

Non-Newtonian fluid barrier

Waterjets & microturbines

Electro-fulguration

Mechanical rotary cutters

Dye-mediated laser ablation

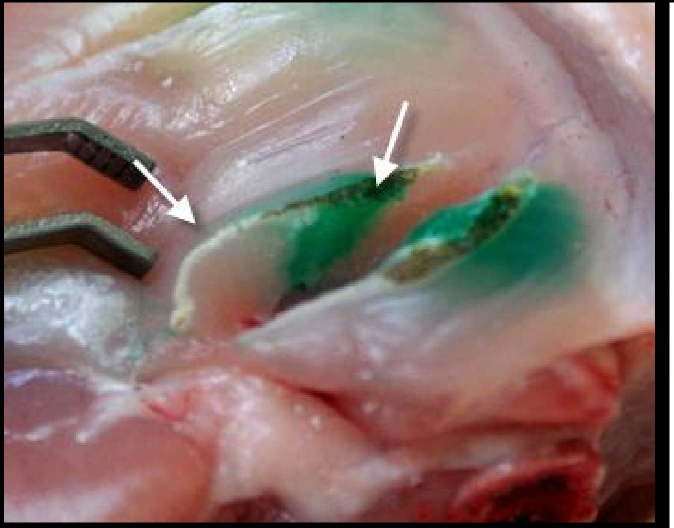

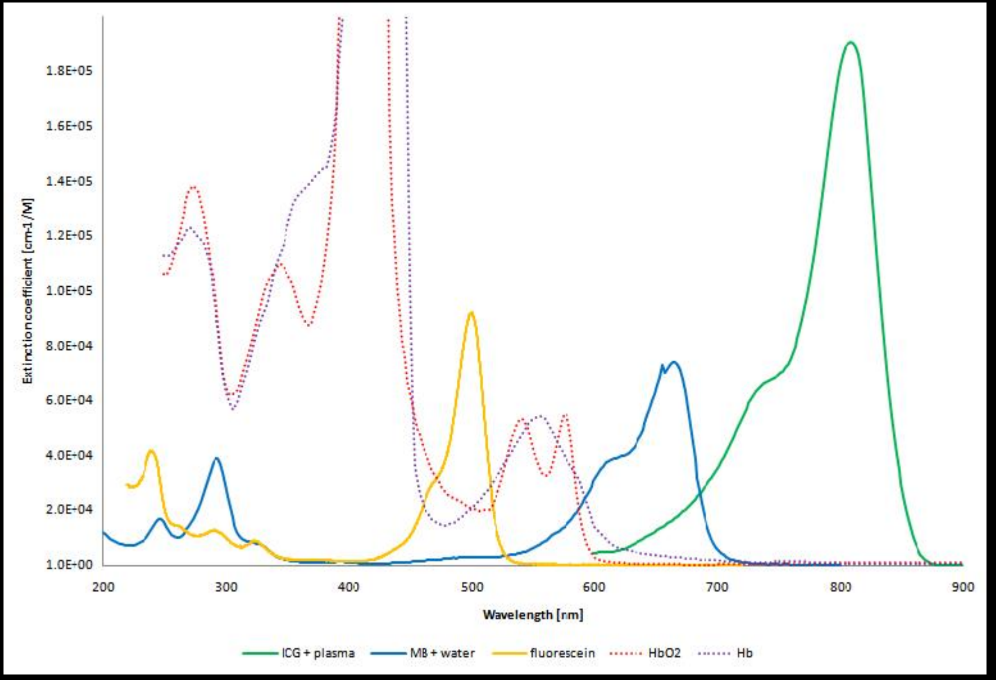

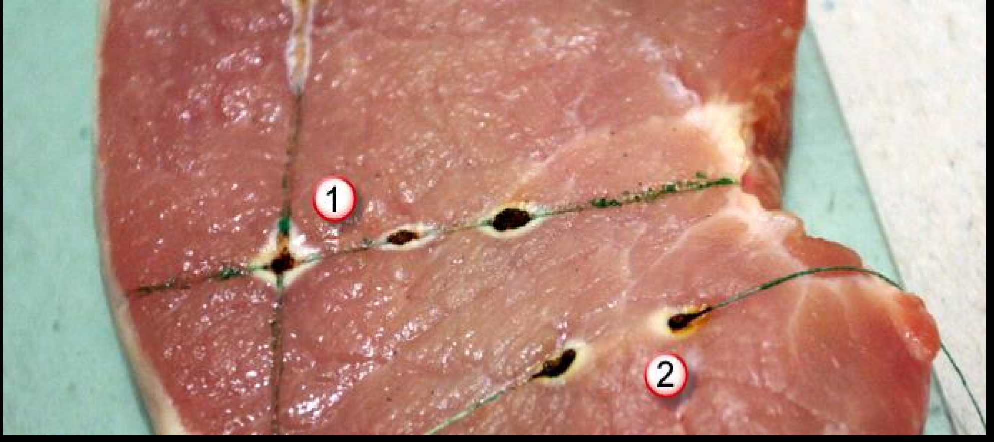

Dye	Laser	Result (dye concentration, runs)
-	Carbon dioxide 10.6 µm laser (30 W maximum)	Ablation (n=5)
-	Diomed 805 nm laser (25 W maximum)	No effect (n=5)
Indocyanine green	Diomed 805 nm laser (25 W maximum)	Ablation (n=10)
Methylene blue	Diomed 805nm laser (25 W maximum)	Ablation* (5 mg/ml, n=5)
-	Diomed 652 nm PDT laser (2 W maximum)	No effect (n=3)
Methylene blue	Diomed 652 nm PDT laser (2 W maximum)	Coagulation (1mg/ml , n=5) Ablation (11mg/ml , n=3, t >> 9.9 s)

Tissue	Water, %	Ash, %	Lipid, %	Protein, %
Whole body	60	4.8-5.8	19 (5.3)	15-30
Blood	79.0-80.8	1.0	0.65	18-19
Fatty, adipose	[11.4-30.5] (21.2)	0.3	[61.4-87.3] (71.4)	[1.0-7.9] (4.4)
Intestine	77.4-82.2 (79)	0.4-1.3 (0.8)	1.3-9.2 (6.2)	10.9-14.9 (13)
Kidney	[72.3-80.5]	0.9	[2.8-6.9] (4.8)	[15.8-19.9] (17.7)
Liver	[72.8-75.6] (74.5)	1.2	[1.5-7.8] (4.6)	[16.1-19.6] (17.6)
Muscle (skeletal)	[70.0-78.6] (74.1)	1.0	[1.6-6.8] (4.2)	[17.9-21.3] (19.8)
Oesophagus	76	0.5-1.1 (0.9)	...	...
Skin	[58.6-72.1] (65.3)	0.7	[5.2-13.5] (9.4)	[22.0-27.2] (24.6)
Stomach	60-78 (75)	0.8	6.2	17.0

(Selected data compiled from Duck 1990.)

Very selective effect. Promising concept.

Selective tissue stiffening

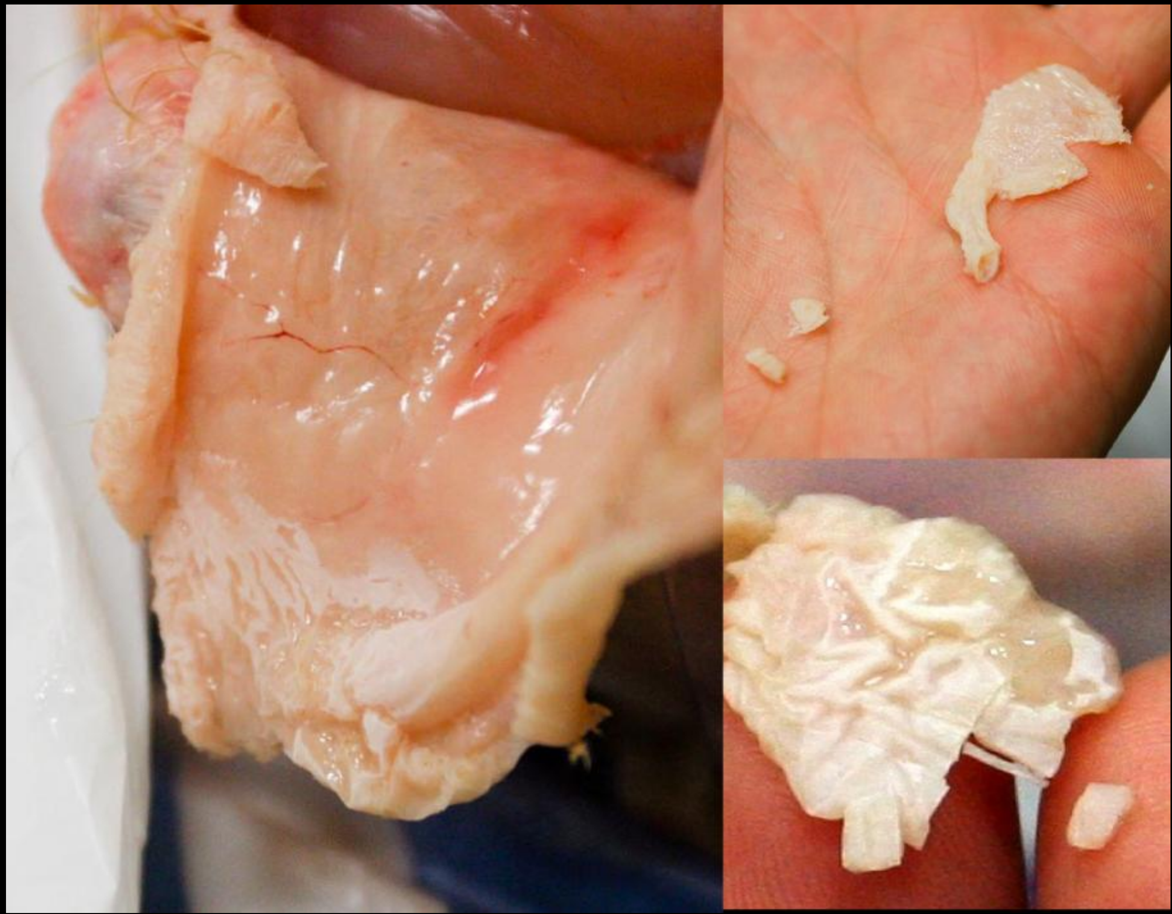

Material	Young's modulus, E	Toughness, G_c	Fracture toughness, K_c
Chicken skin	15-60 kPa [278]	2.8 KJ/m² [277]	6.5-13.0 kN $m^{-3/2}$
Cyanoacrylate	1.17 GPa [279]	1.6 kJ/m² [280]	1.4 MN $m^{-3/2}$

Skin is about 2x tough as CA,
but stiffness is lower by almost 5 fold.

Crack propogation with scissors

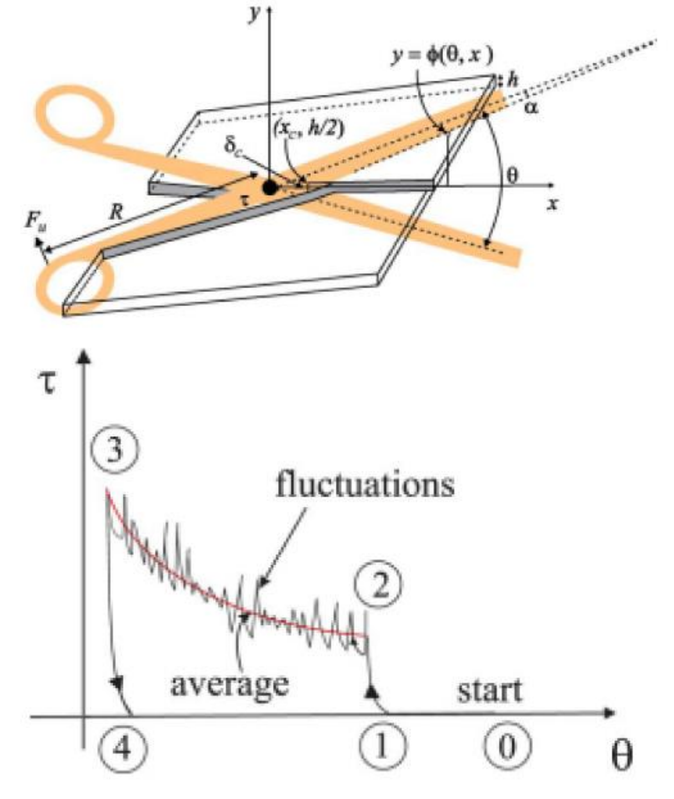

(Reproduced from Mahvash et al. 2008)

Clinically promising, but not very interesting scientifically.

Beam Theory

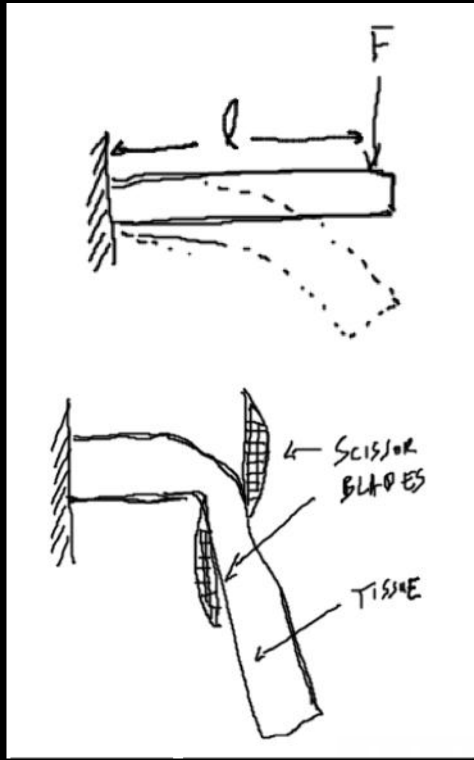

$$\theta = \frac{Fl^2}{C_2 EI}$$

$$\delta = \frac{Fl^3}{C_1 EI}$$

Fracture Mechanics

$$\boxed{K_c = \sigma\sqrt{\pi a}} = \sqrt{EG_c} \qquad \sigma = E\varepsilon$$

Blunt dissection by chemical reaction

$$NaHCO_3(aq) + CH_3COOH(aq) \rightarrow NaC_2H_3O_2(aq) + H_2CO_3(aq)$$

$$H_2CO_3(aq) \rightarrow H_2O(l) + CO_2(g)$$

Baking Soda + Tap Water

\+

Vinegar

=

Gas!

Pseudo-first order chemical rate equation

$$A + B \rightarrow C$$

$$r = -\frac{d[A]}{dt} = k[A], ([B] \gg [A])$$

$$A = A_0 e^{-kt}$$

Arrhenius equation

$$k = Ae^{-E_a/RT}$$

None of the test cases in either stomach (n=2) nor oesophagus (n=2) resulted in any visible delamination of tissue layers.
Control cases (n=4) also were negative for delamination or dissection.

Not very promising for tissue dissection.
But foamy mixture might be good for EMR or ESD.

Non-Newtonian fluid barrier

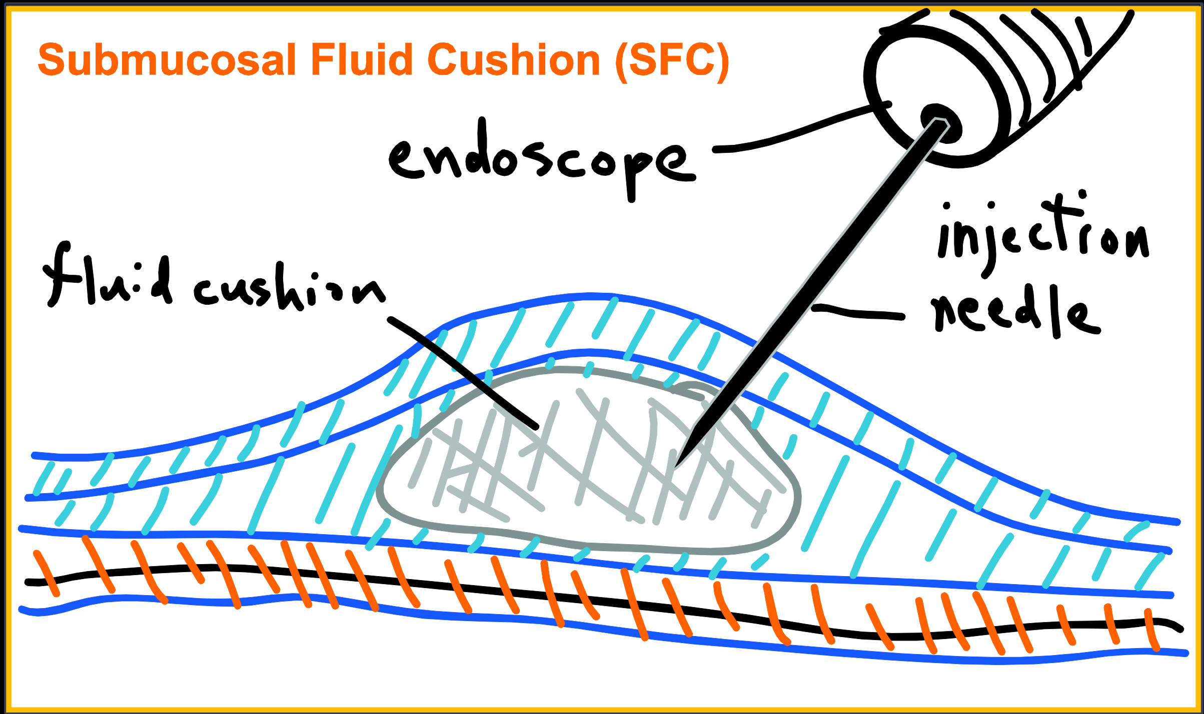

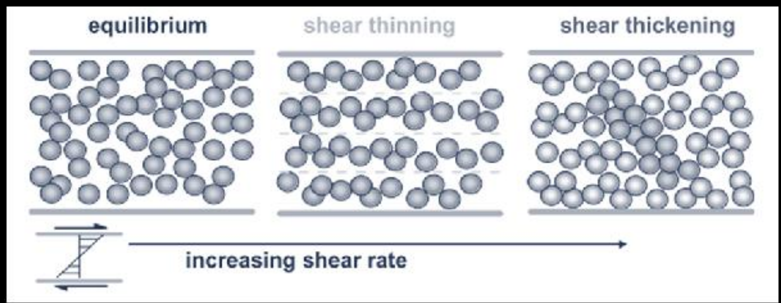

(Reproduced from Wetzel et al. 2003)

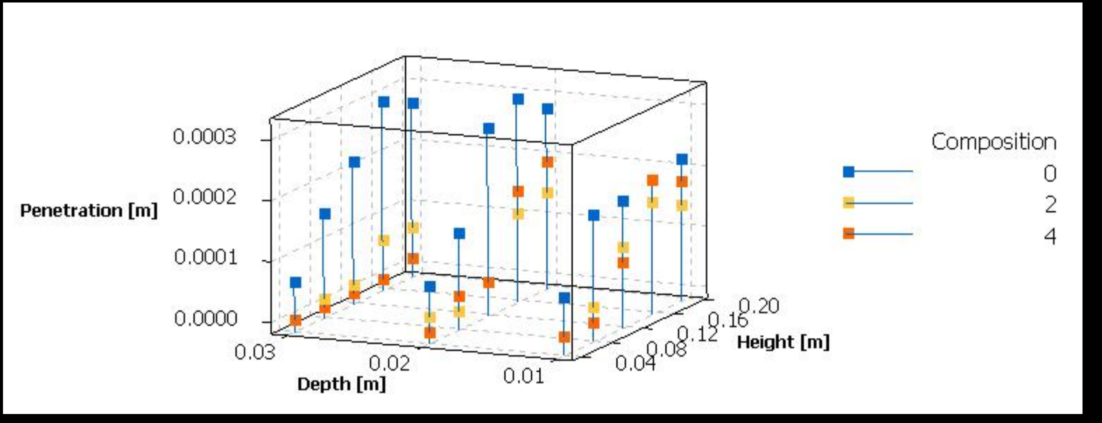

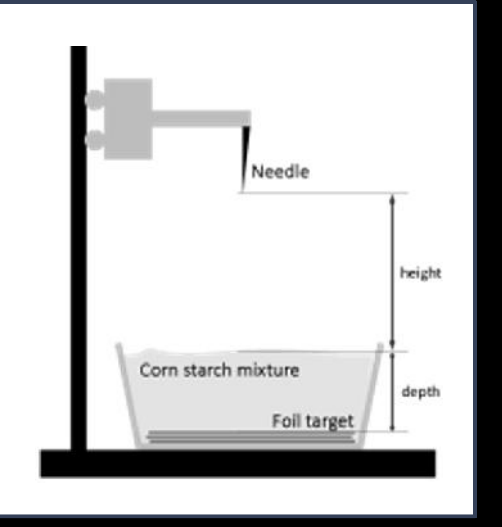

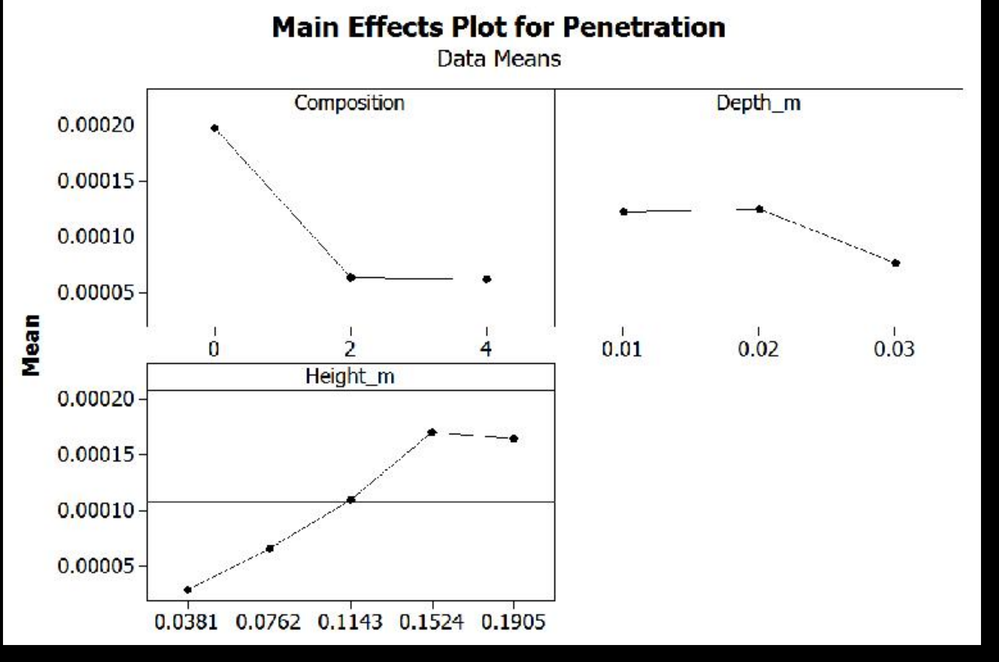

Some protection offered, but future uncertain.

Mono- & bipolar electrofulguration

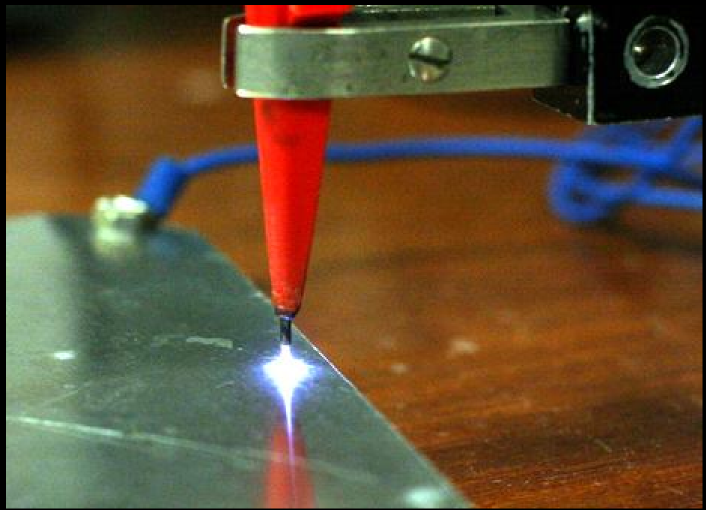

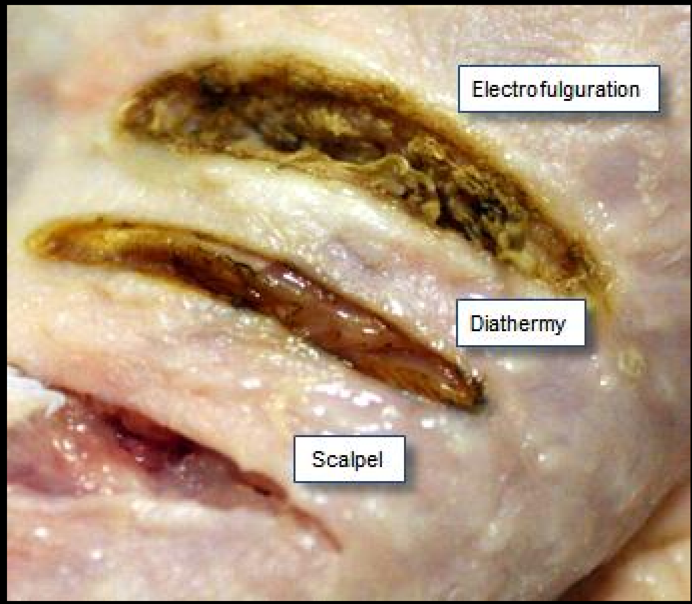

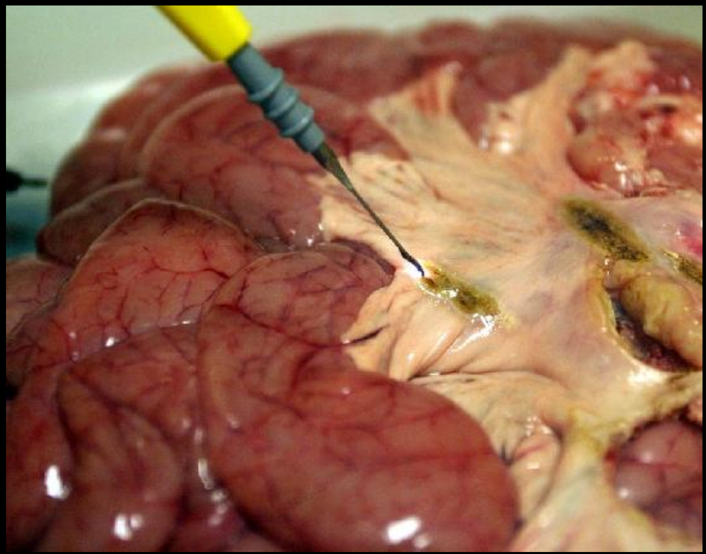

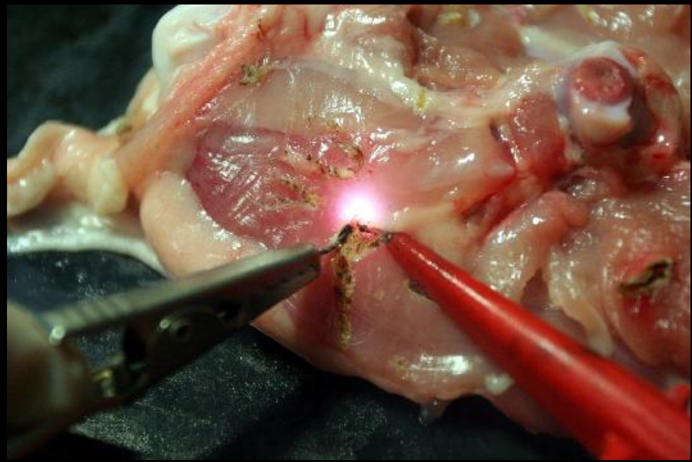

Promising cutting performance.
However, two commercial devices were introduced to market during research.

Conductive / insulating masks

“Rubber tires” and “lightning rods”

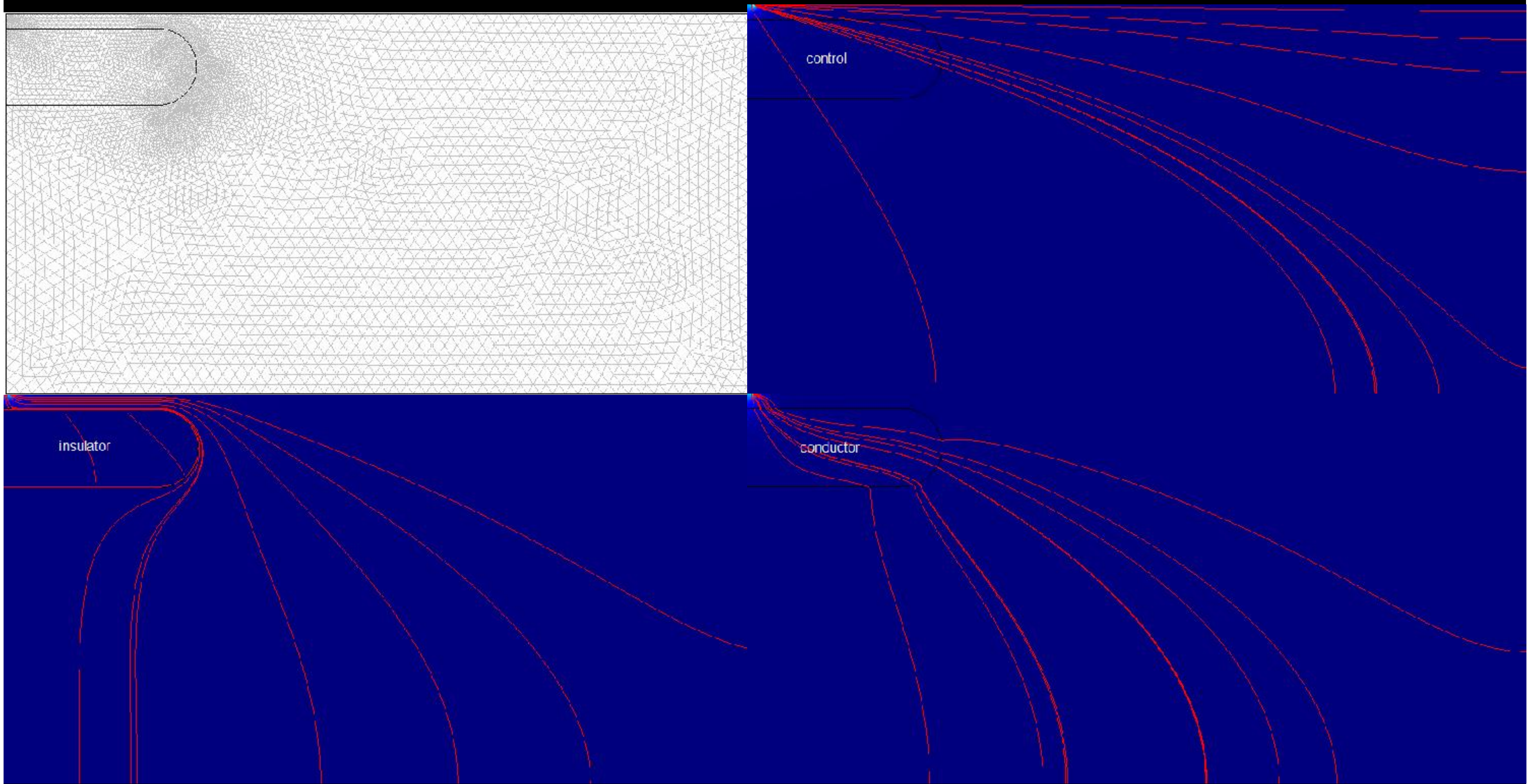

Theoretical simulations were interesting.
Overall research topic too uncertain.

Miscellaneous ideas (not evaluated)

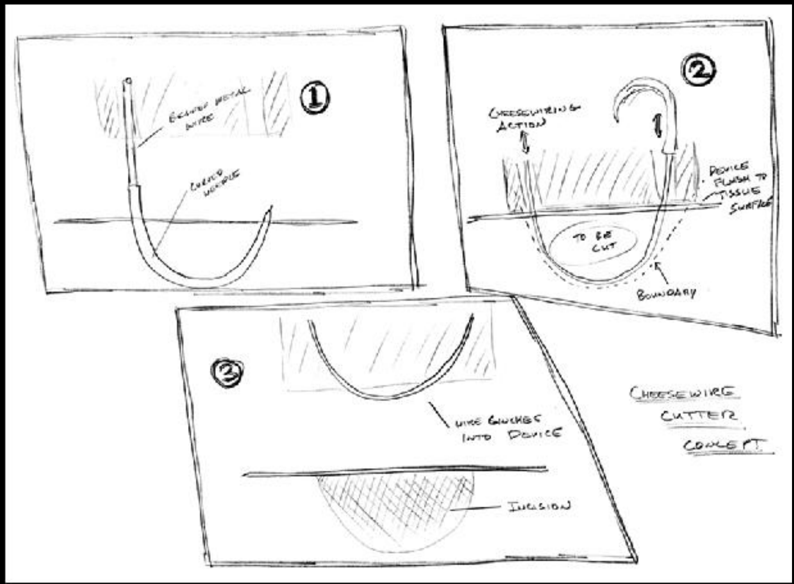

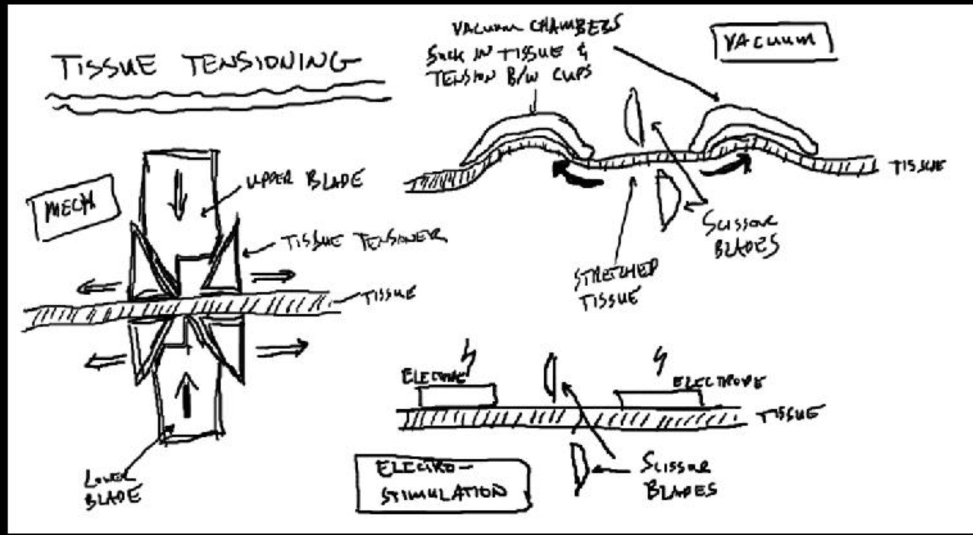

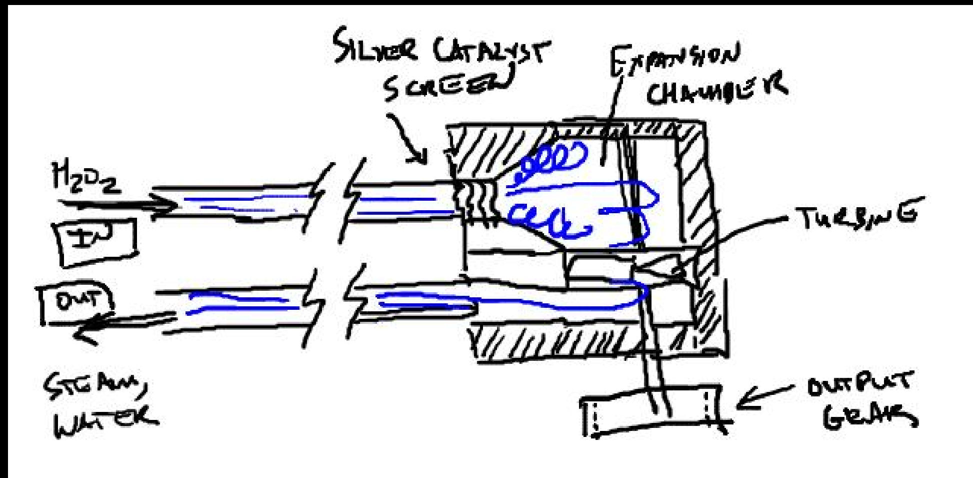

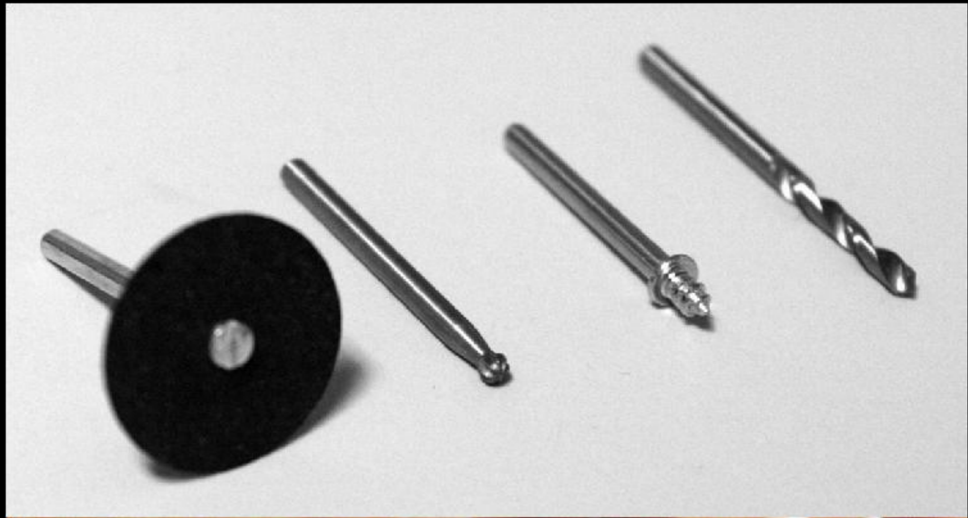


Sensitization Tactic

- Dye-mediated laser ablation
- Selective tissue stiffening with glue
- Blunt dissection by gas-evolving chemical reaction

Protection Tactic

- Non-Newtonian fluid barrier
- Conducting or insulating masks for RF-energy

Other

- Monopolar & bipolar electro-fulguration
- Circular and rotary saw

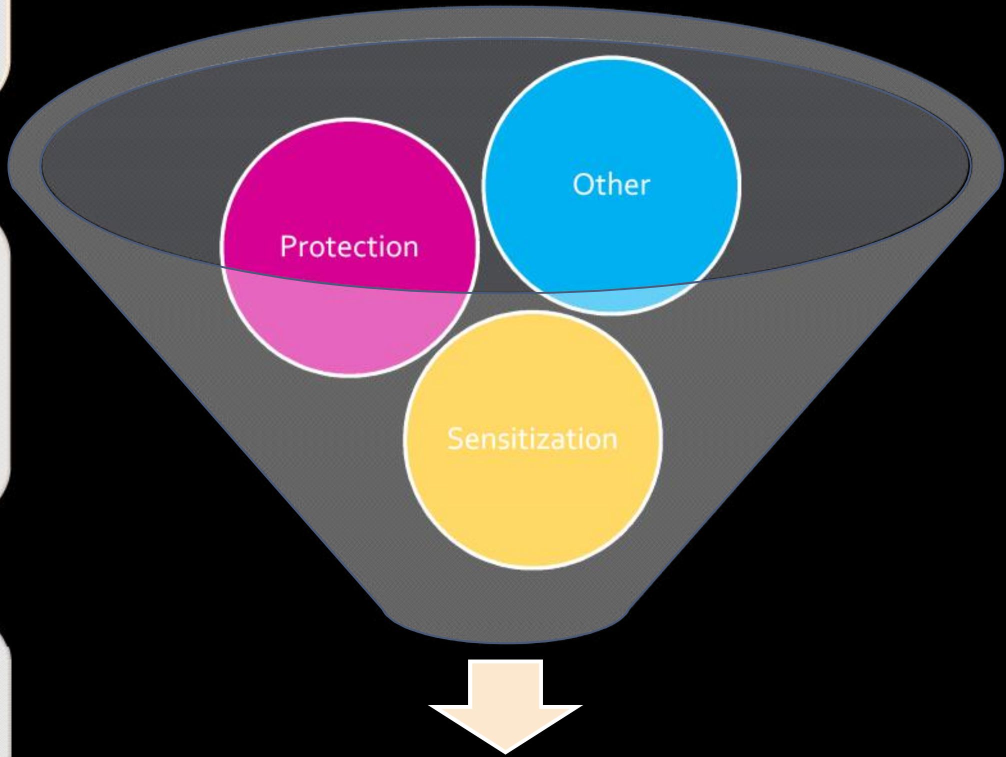

Dye-mediated laser ablation

How can we improve control?

Dye-mediated laser ablation

The Laser

Diomed 25 Laser, 25 W laser light at 805 nm.
Often used clinically in interstitial laser photocoagulation (ILP).
Also used in research for ablating tissue by using a 300 µm fibre in contact mode.

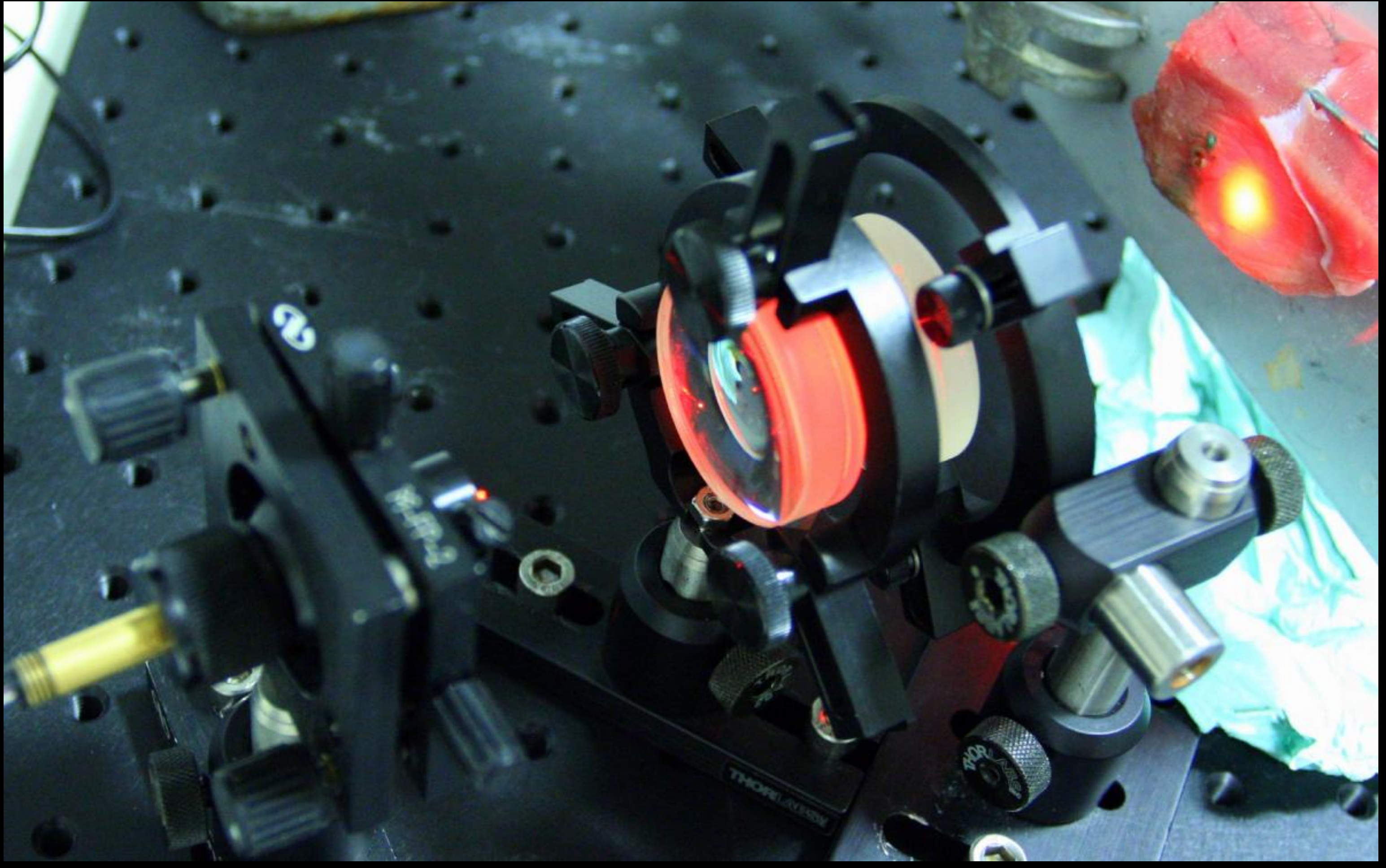

Power calibration

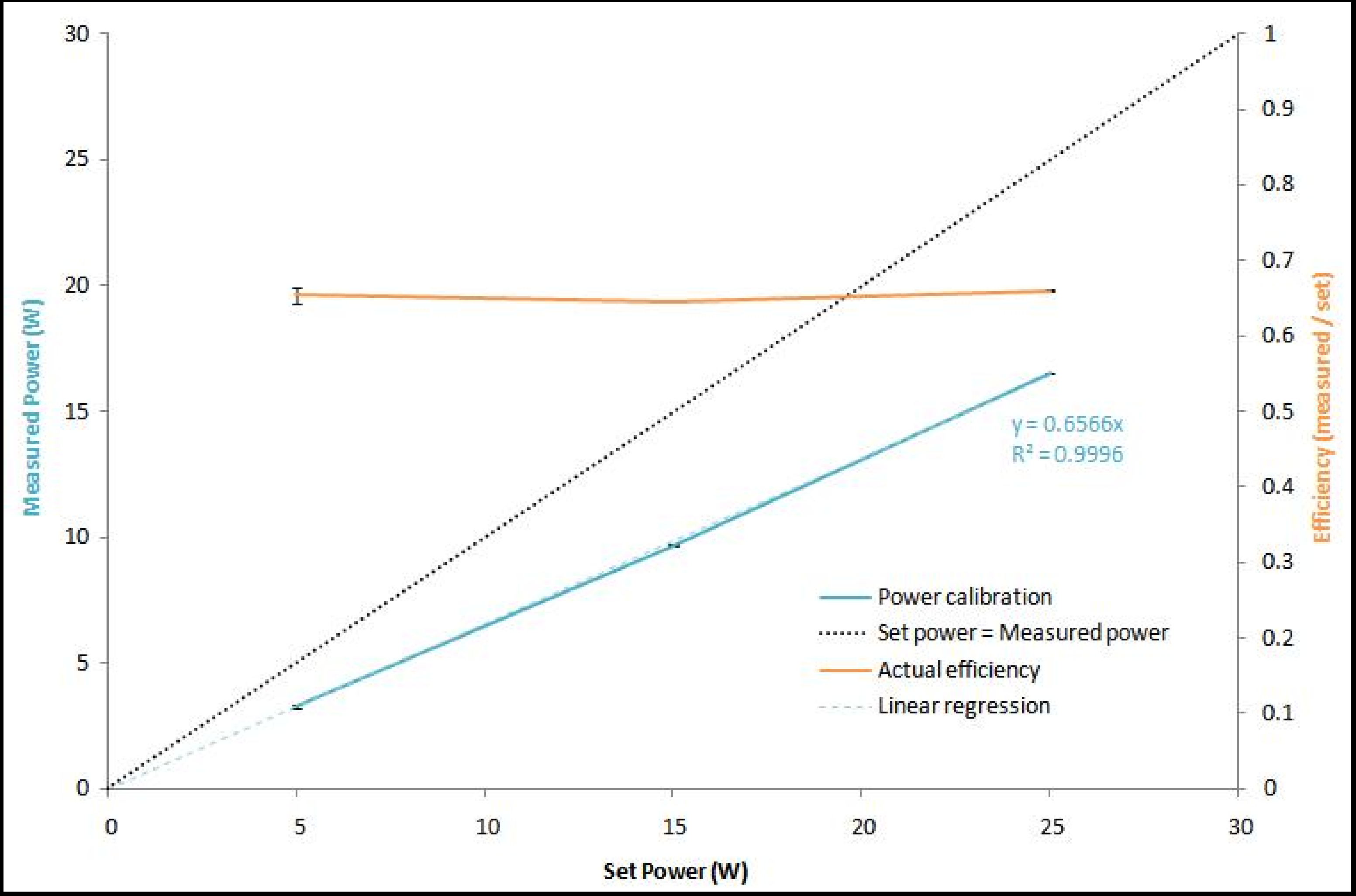

Calibration of the set power vs. measured output power for the Diomed 25 laser (n=28). Error bars are standard errors. The overall laser system with the fibre and mode scrambler has an output efficiency of ~66%.

Beam profile

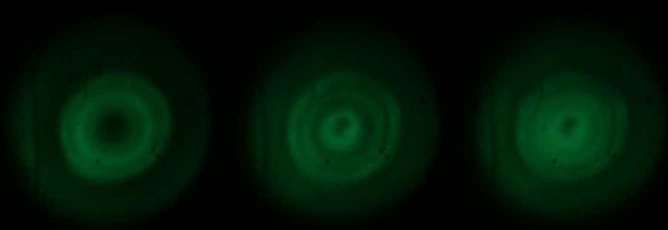

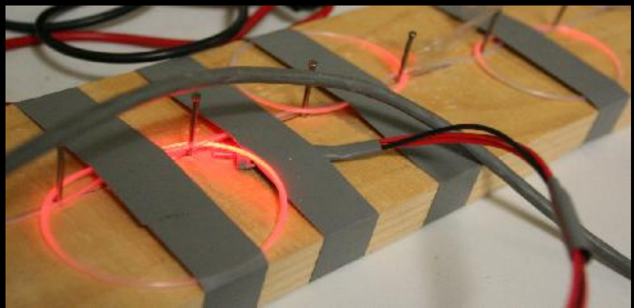

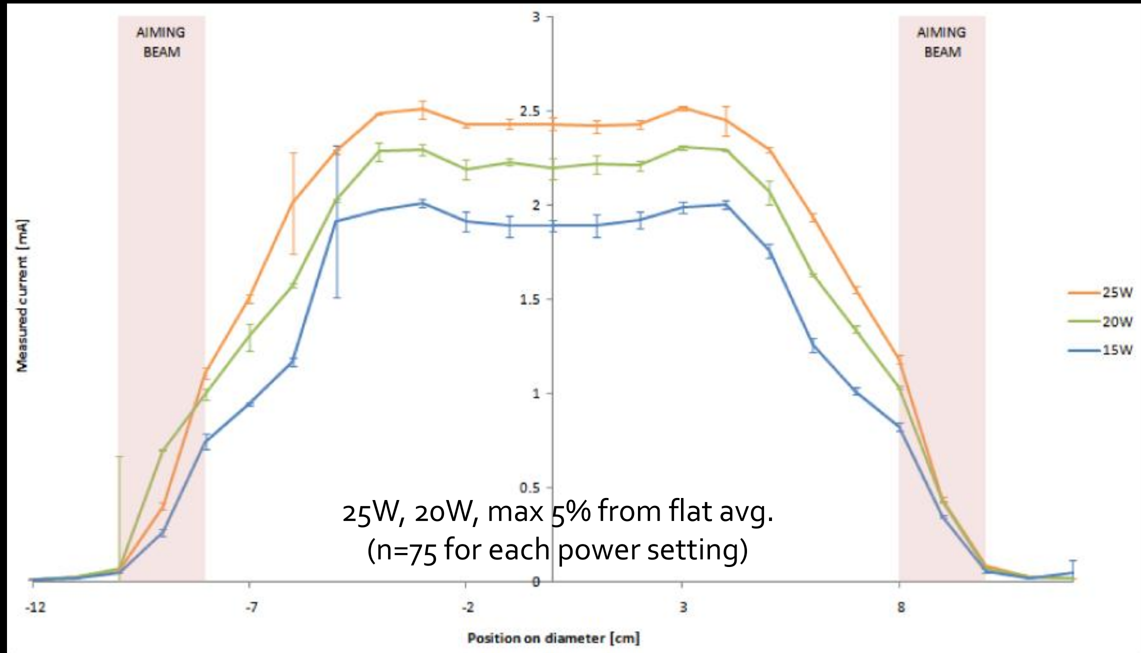

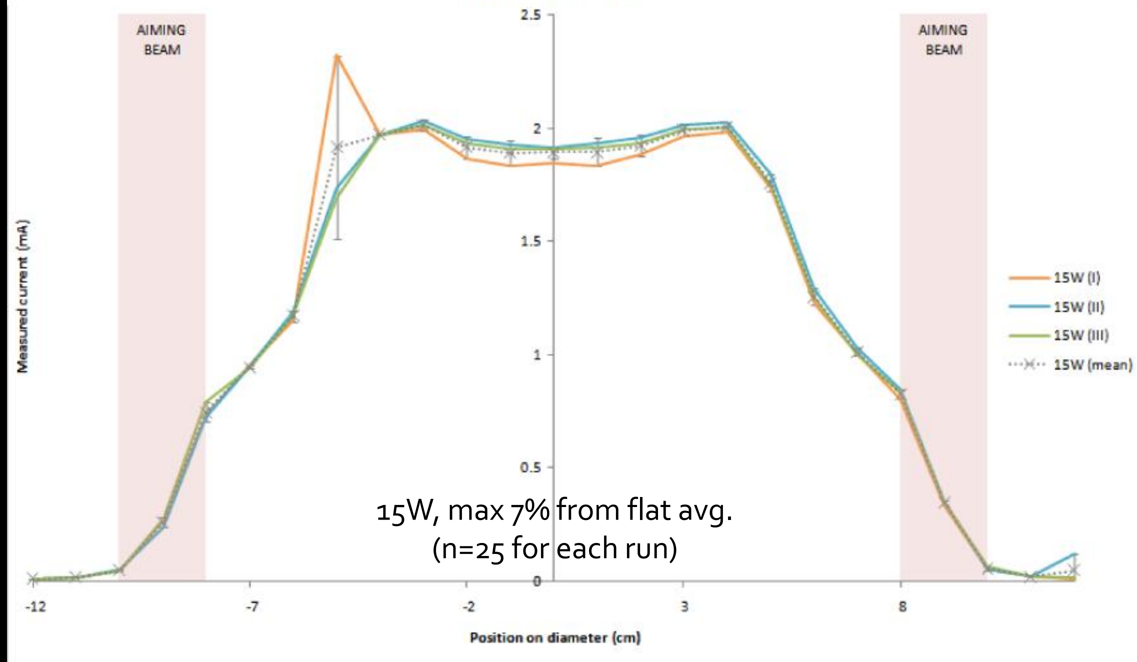

Beam divergence

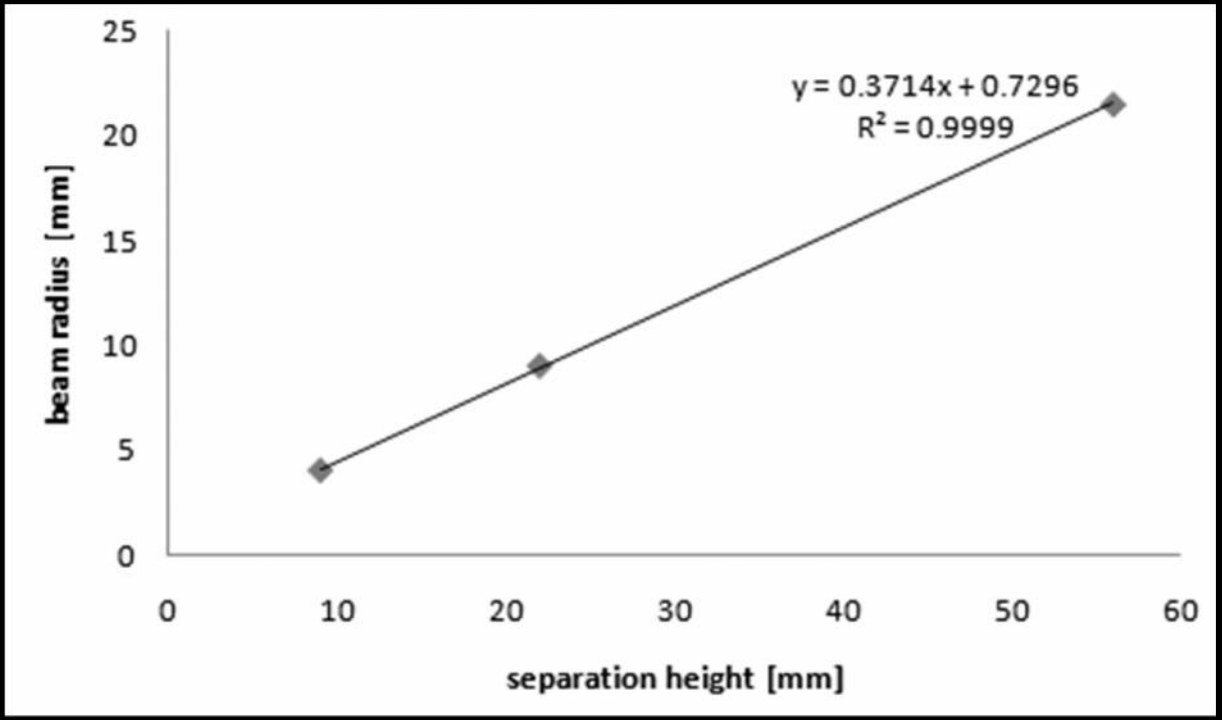

beam divergence of 20.4 degrees

Laser wavelength

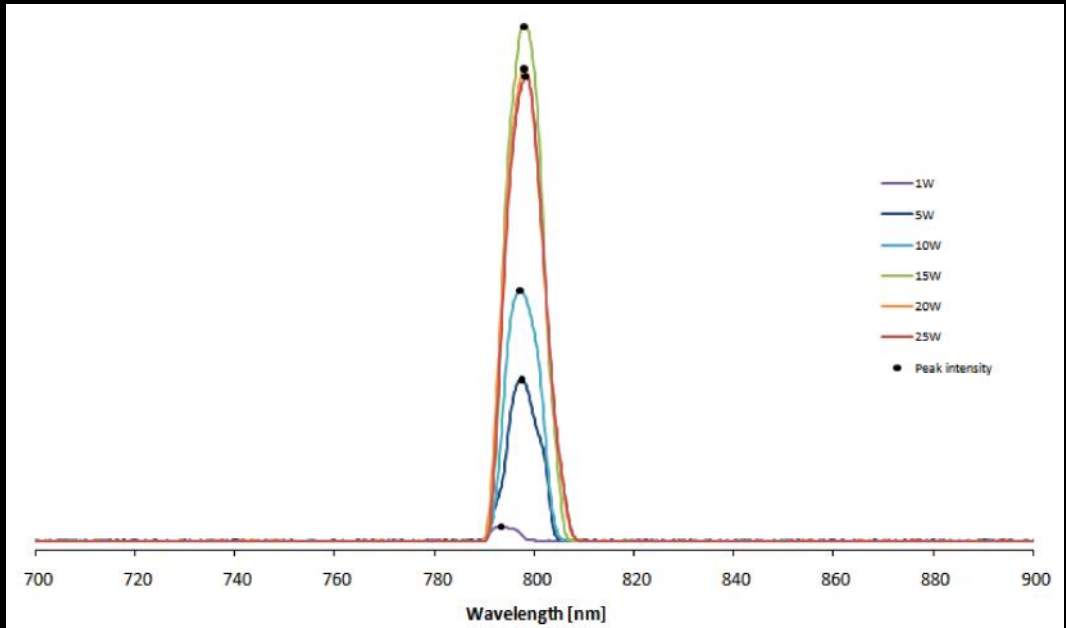

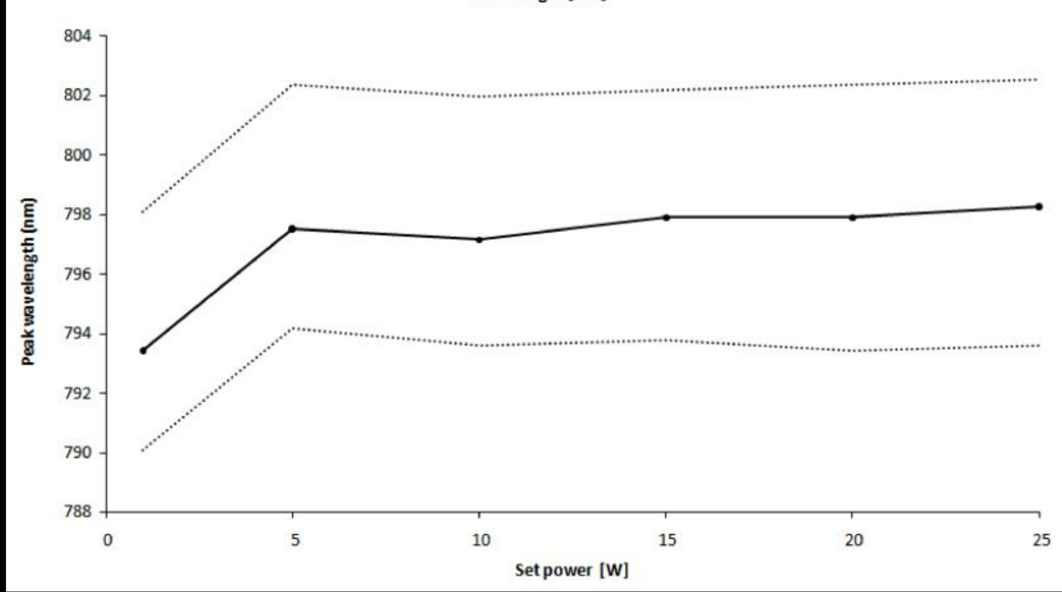

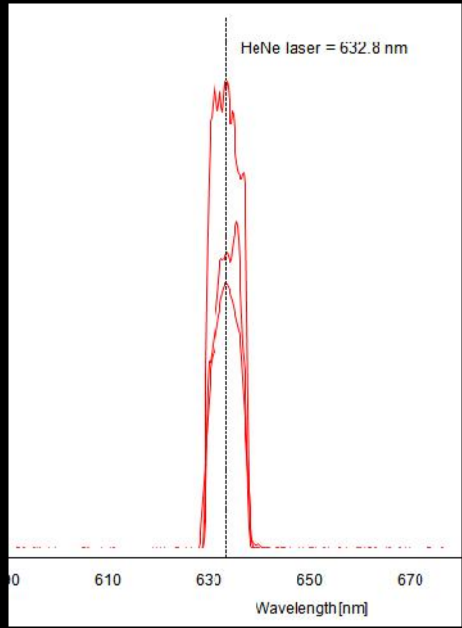

Slight increase in wavelength with power. But less than spectrometer ability to resolve wavelength.

Dependence probably non-existent or insignificant.

The Dye

Indocyanine green.

$C_{43}H_{47}N_2O_6S_2Na$ is a tricarbocyanine dye with molecular weight of 775.

Has a long history of clinical use.

Administered routinely as a contrast agent for measuring perfusion in ocular vasculature, blood volume, cardiac output and hepatic function.

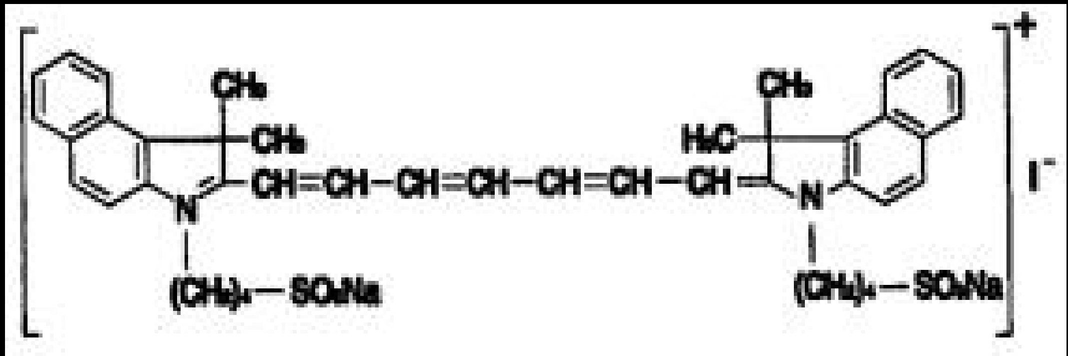

Absorption Spectra (ICG/BSA)

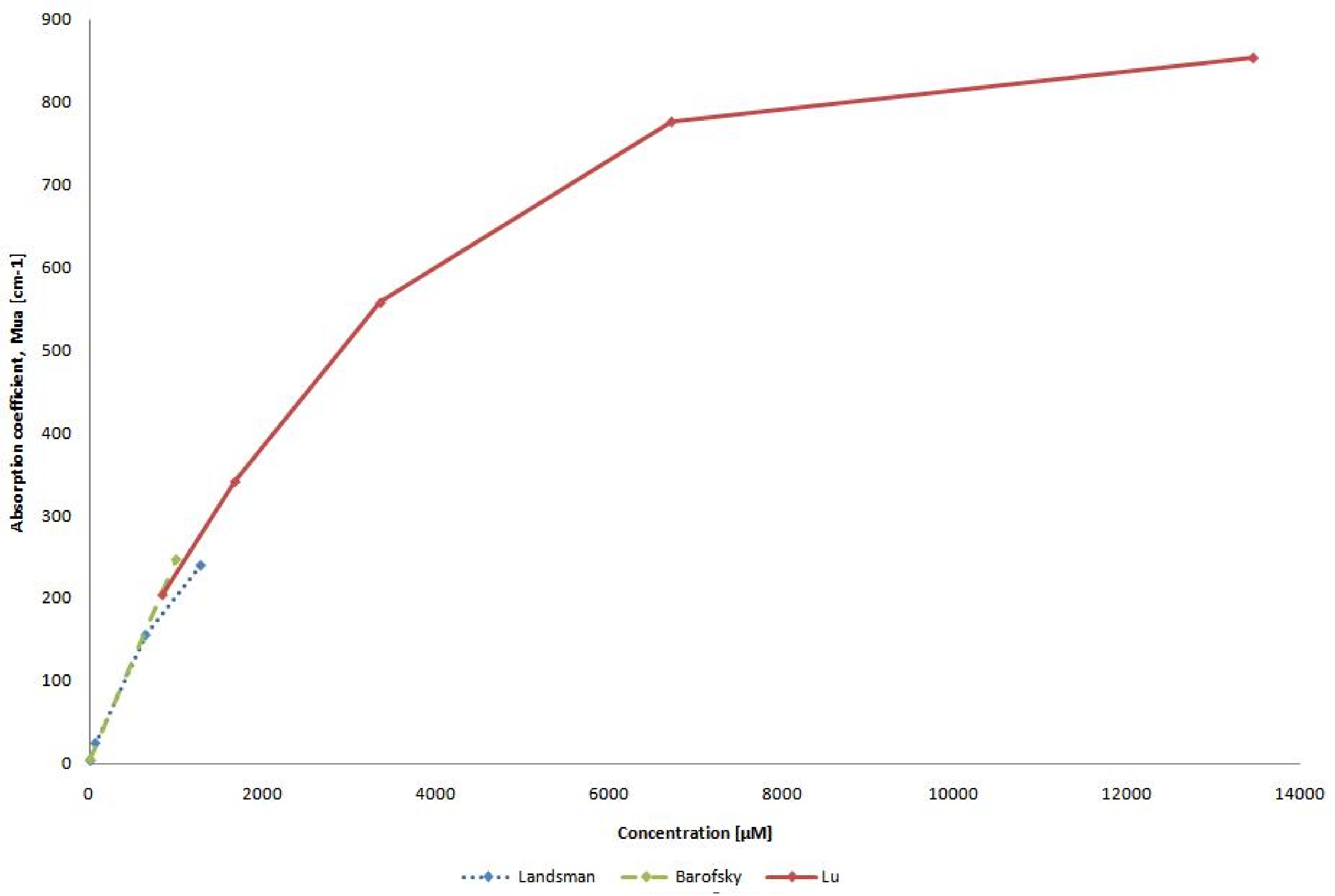

Absorption Spectra (ICG/H_2O)

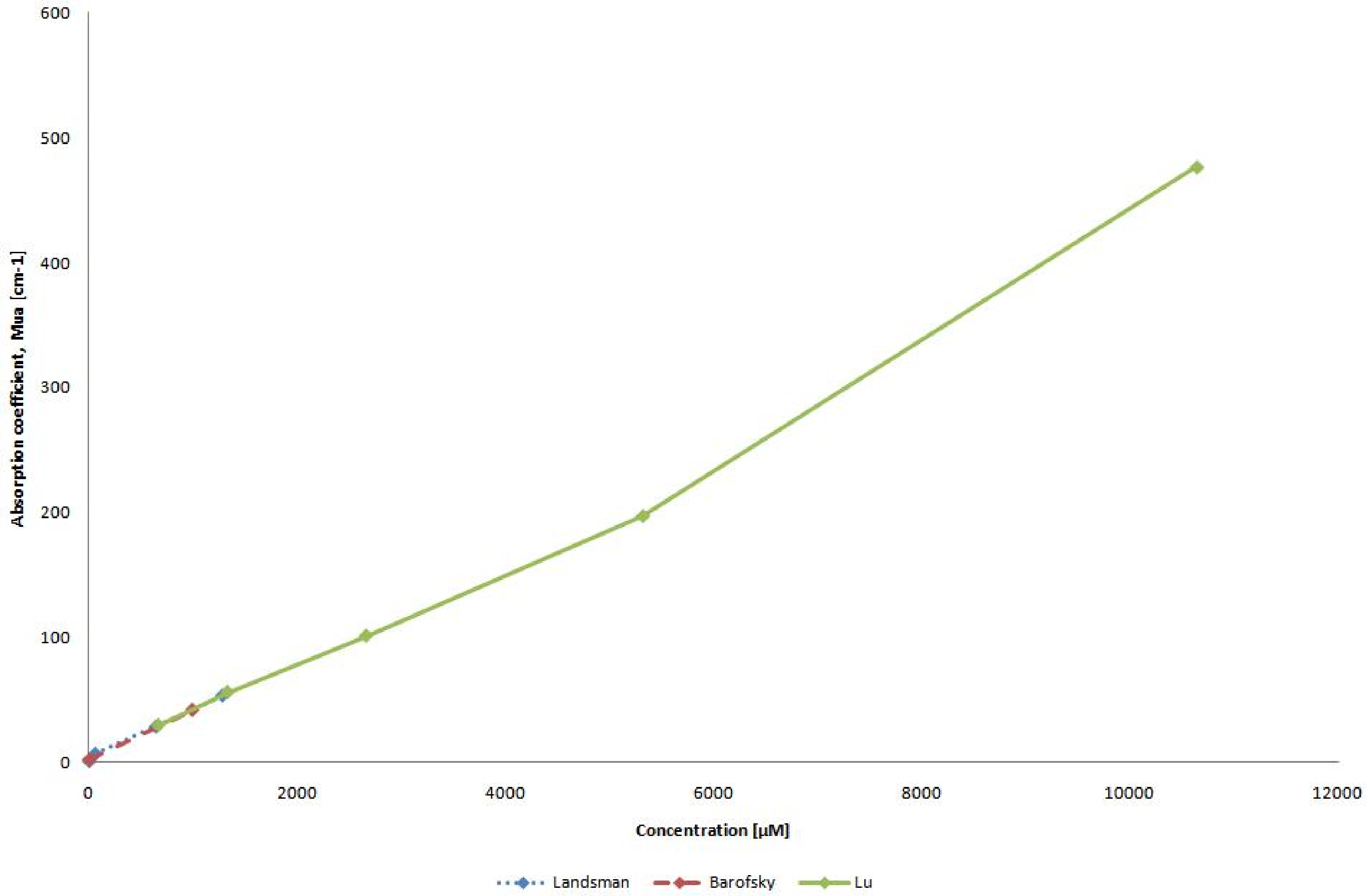

Diffusion into tissue

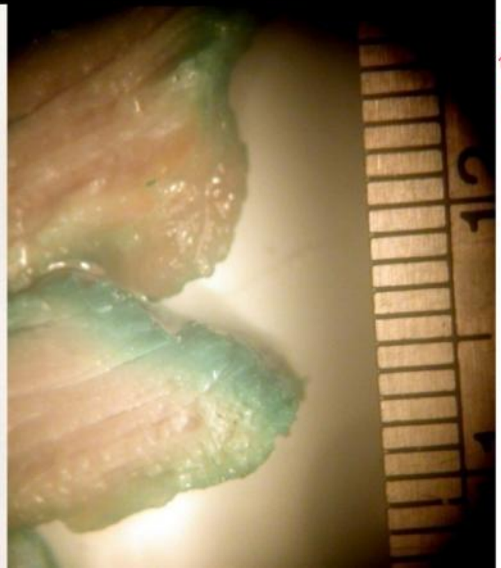

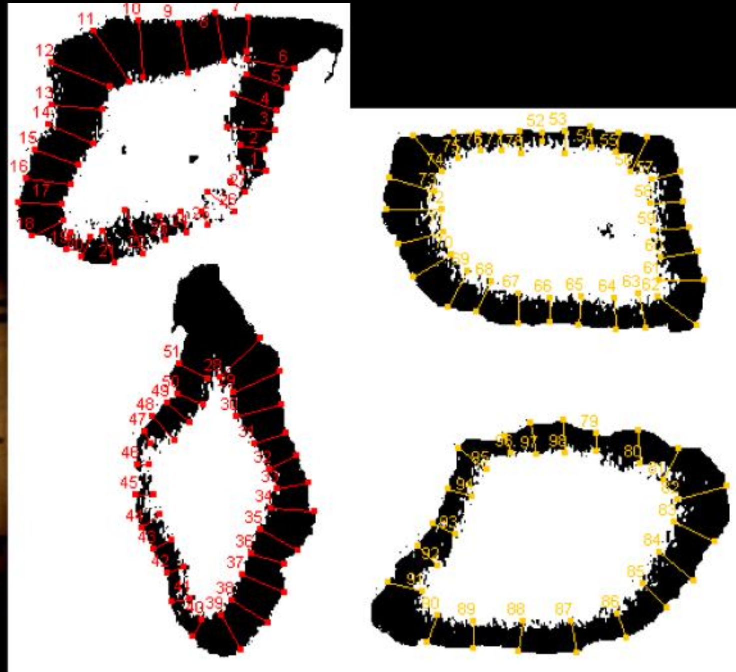

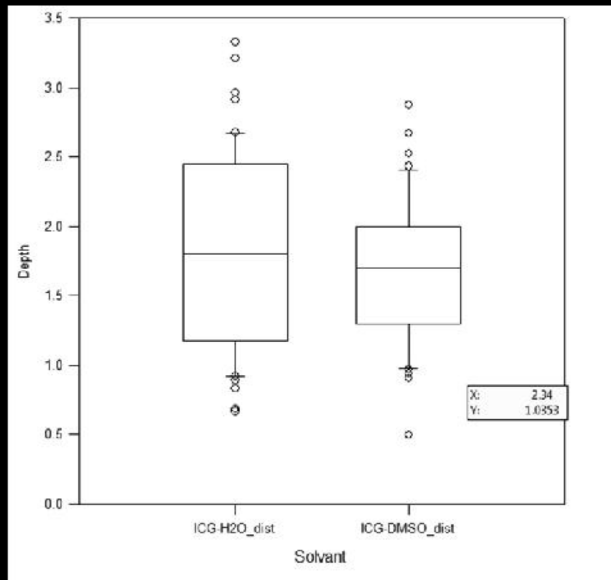

Fick's Second Law of Diffusion & 1D solution

$$\frac{\partial \varphi}{\partial t} = D\frac{\delta^2 \varphi}{\partial x^2} \qquad \frac{n(x,t)}{n(0)} = erfc\left(\frac{x}{2\sqrt{Dt}}\right)$$

After 5 mins diffusion time,
diffusion depth is 0.11 mm.

Lateral spread of dye

Dye volume	After 5 s, mean area (std. error)	After 15 s, mean area (std. error)
1 µl	10.9 mm² (1.2) (n=10)	11.7 mm² (1.4) (n=10)
3 µl	21.1 mm² (0.8) (n=10)	22.3 mm² (0.8) (n=10)
5 µl	29.0 mm² (1.7) (n=10)	30.2 mm² (2.3) (n=10)

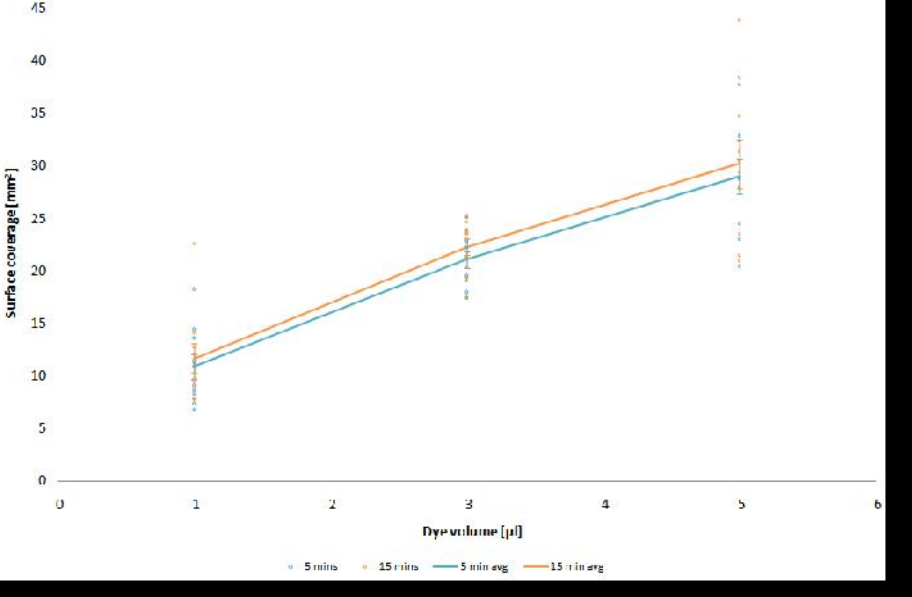

Dye Volume	1 µl	3 µl	5 µl
Thickness	85.5 µm	134.5 µm	165.6 µm

In vivo, porcine model

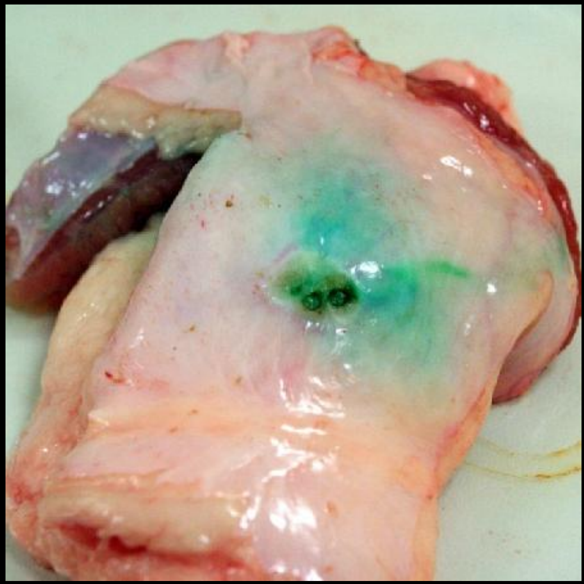

It works!

Theoretical model of laser ablation

- McKenzie 1983: Extent of thermal damage beneath CO_2 laser ablation craters
- Welch 1984: Reviewed various methods to model light and heat distribution in laser irradiated tissue for predicting thermal response of tissue
- Welch et al. 1985: Model of laser angioplasty, included Henrique's damage integral
- Van Gemert et al. 1985: Model of laser angioplasty, 100° C vapourisation point of tissue volume
- McKenzie 1986: 3-damage zone model of CO2 ablation
- Jacques & Prahl 1987: 1D model with diffusion model for LT, heat transport & tissue coagulation by Arrhenius' integral
- McKenzie 1989: Extension to model for Er:YAG, Ho:YAG
- Zhang, Sheng & Zhang 2009: 4-damage zone model

The McKenzie Model

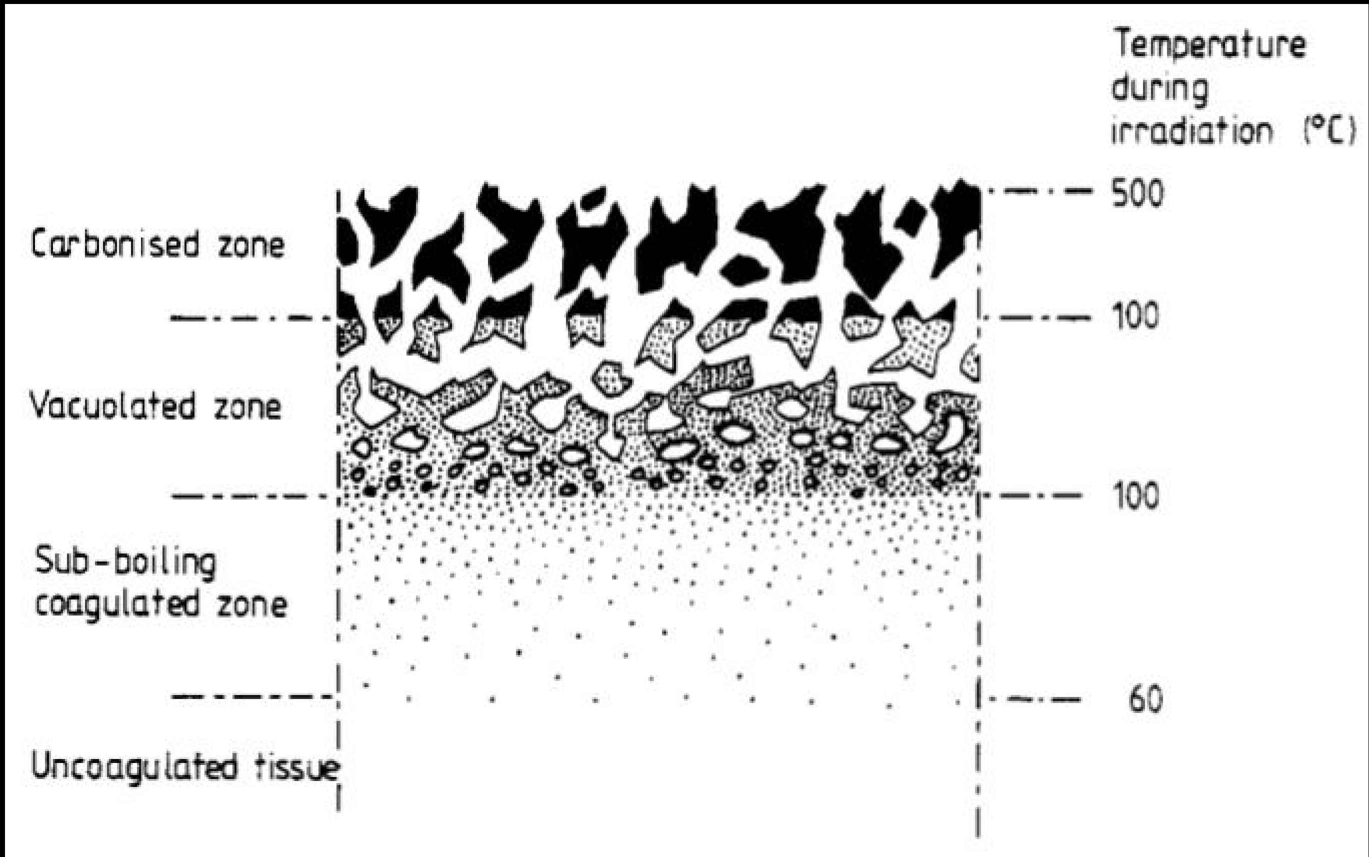

Importance of carbonisation

- **McKenzie 1986:** hinted at importance of carbonisation – one layer in his model. But downplayed contribution due to thinness in CO_2 laser ablation.
- **Verdaasdonk, Borst & van Gemert 1990**: Nd:YAG (10-60 W) and argon (3.5 W) laser ablation of bovine aortic and myocardial tissue.
  Tissue denaturation, explosive vaporisation and cyclic carbonisation.
- **Jacques 1993**: High irradiance ablation of chicken breast muscle by Nd:YAG laser (1064 nm, 90 W, 7mm spot, ~230 W/cm²).

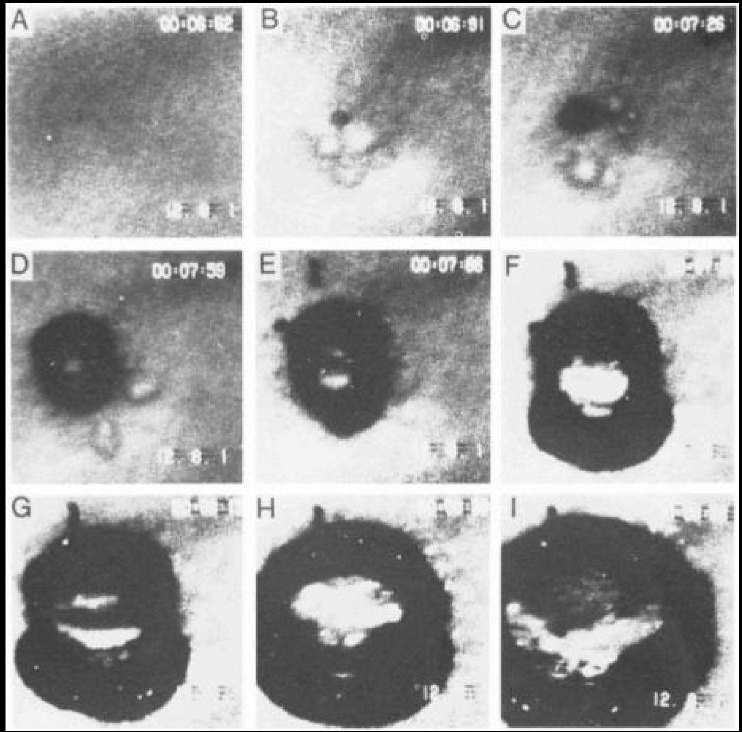

Browning and carbonisation (after 30 s)contributing to high absoption of laser light. "A cycle of removing char and renewing char, which allowed the efficient ablation to proceed at a steady rate."

What happens in dye-mediated laser ablation?

Ablation effects revealed by histology

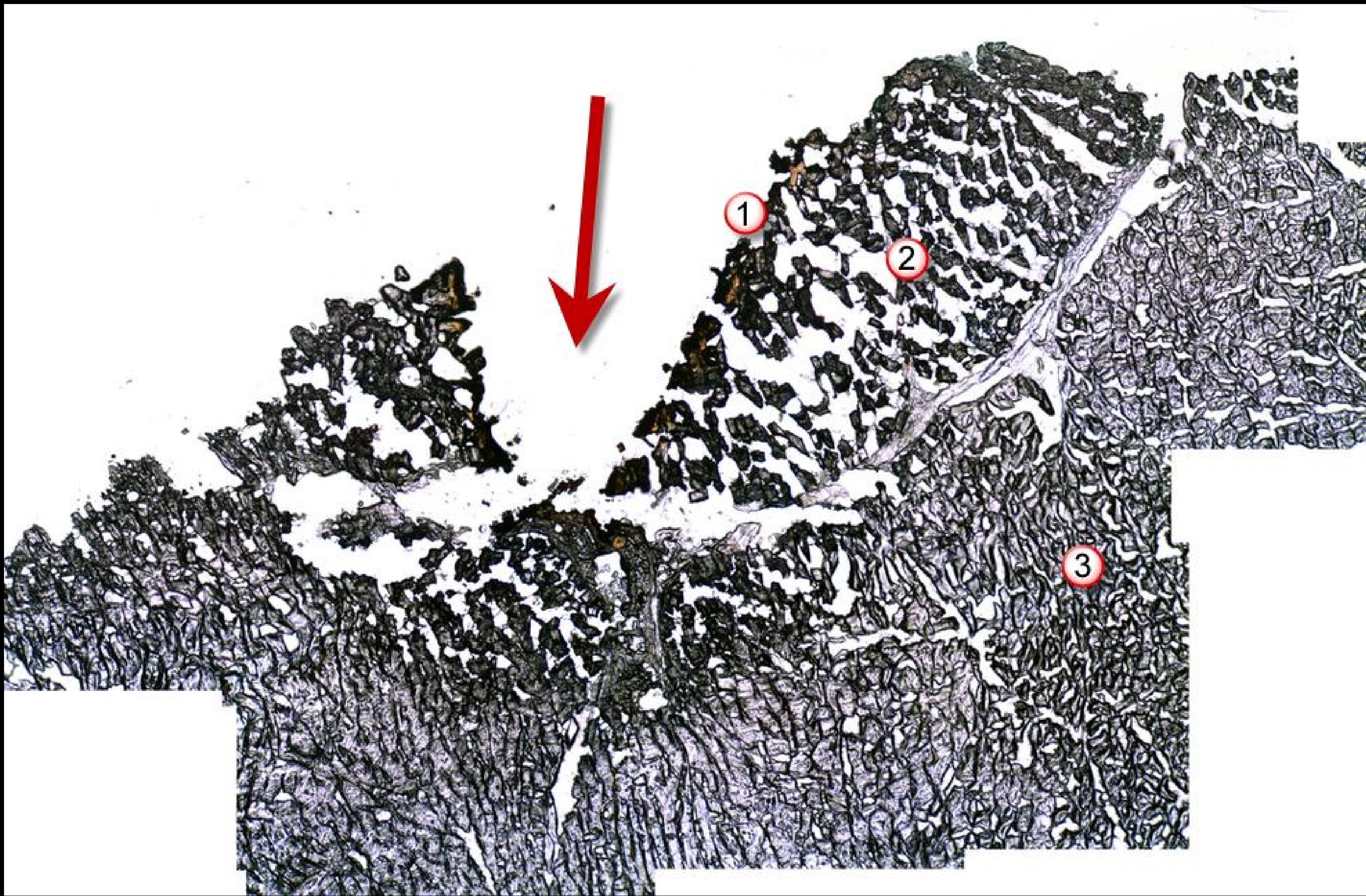

Sequence of events — high speed video

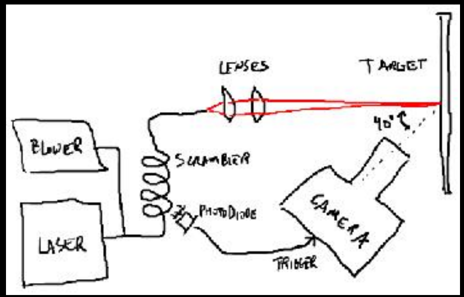

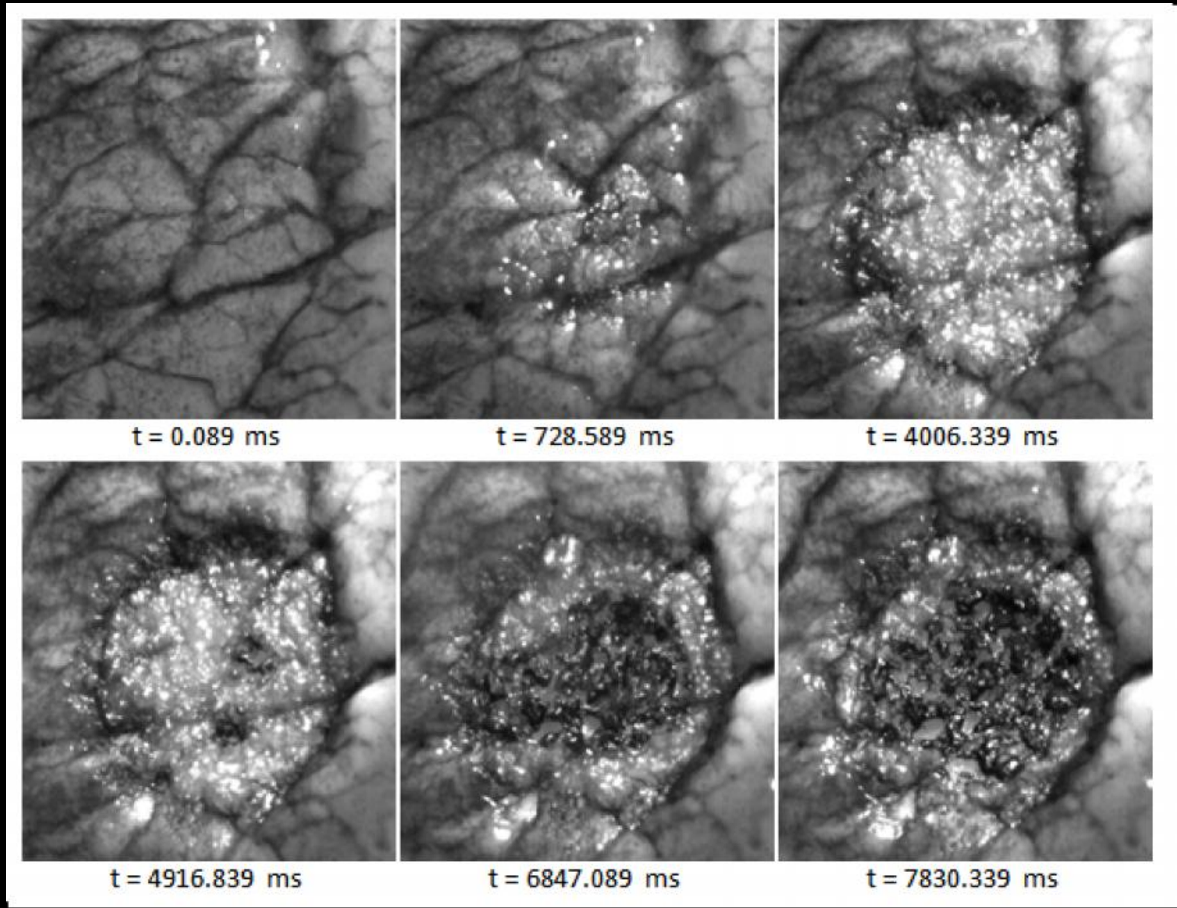

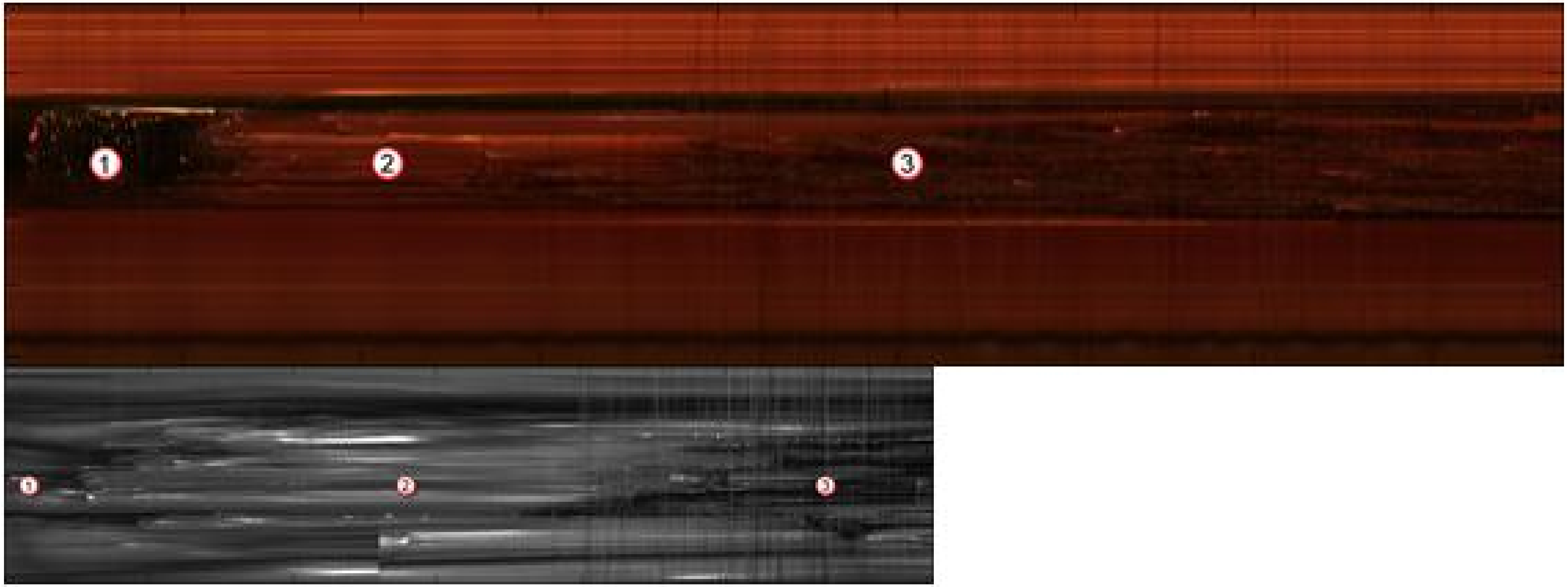

1. Boiling of the pool of dye upon activation of the laser. The boiling was observed to be quite violent, occasionally erupting and sending small droplets of the liquid away from the main pool. During this phase, a whitening of the image can be seen starting from near the centre of the image growing outwards.
2. Disappearance of the dye layer from the centre of the pool outwards to reveal light-coloured, pock-marked tissue underneath.
3. Appearance of small regions of blackened tissue that grow and converge into a single, large blackened area. A large amount of black smoke is generated during this phase of the ablation.

Ablation crater: *en face* video

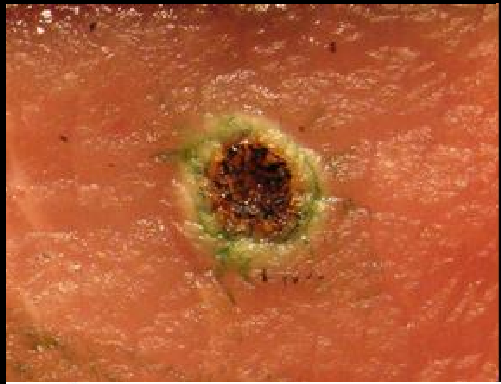

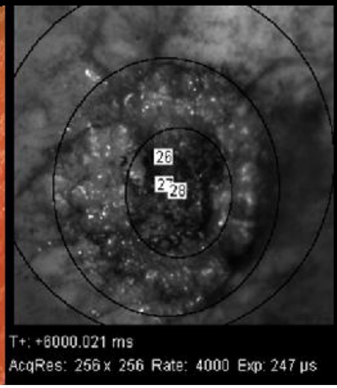

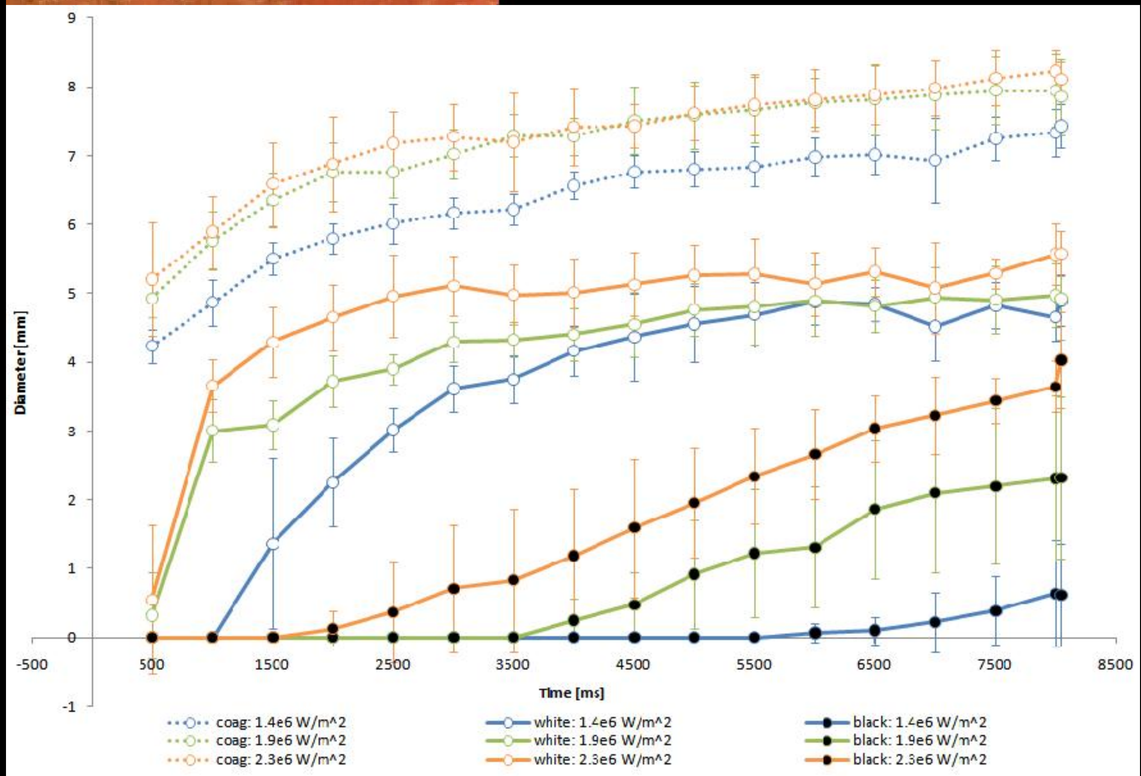

Irradiance	1.4e6 W/m²	1.9e6 W/m²	2.3e6 W/m²
Start time after trigger	6 s	3.5 s	2.0 s
Diameter growth rate	0.3 mm/s	0.5 mm/s	0.6 mm/s

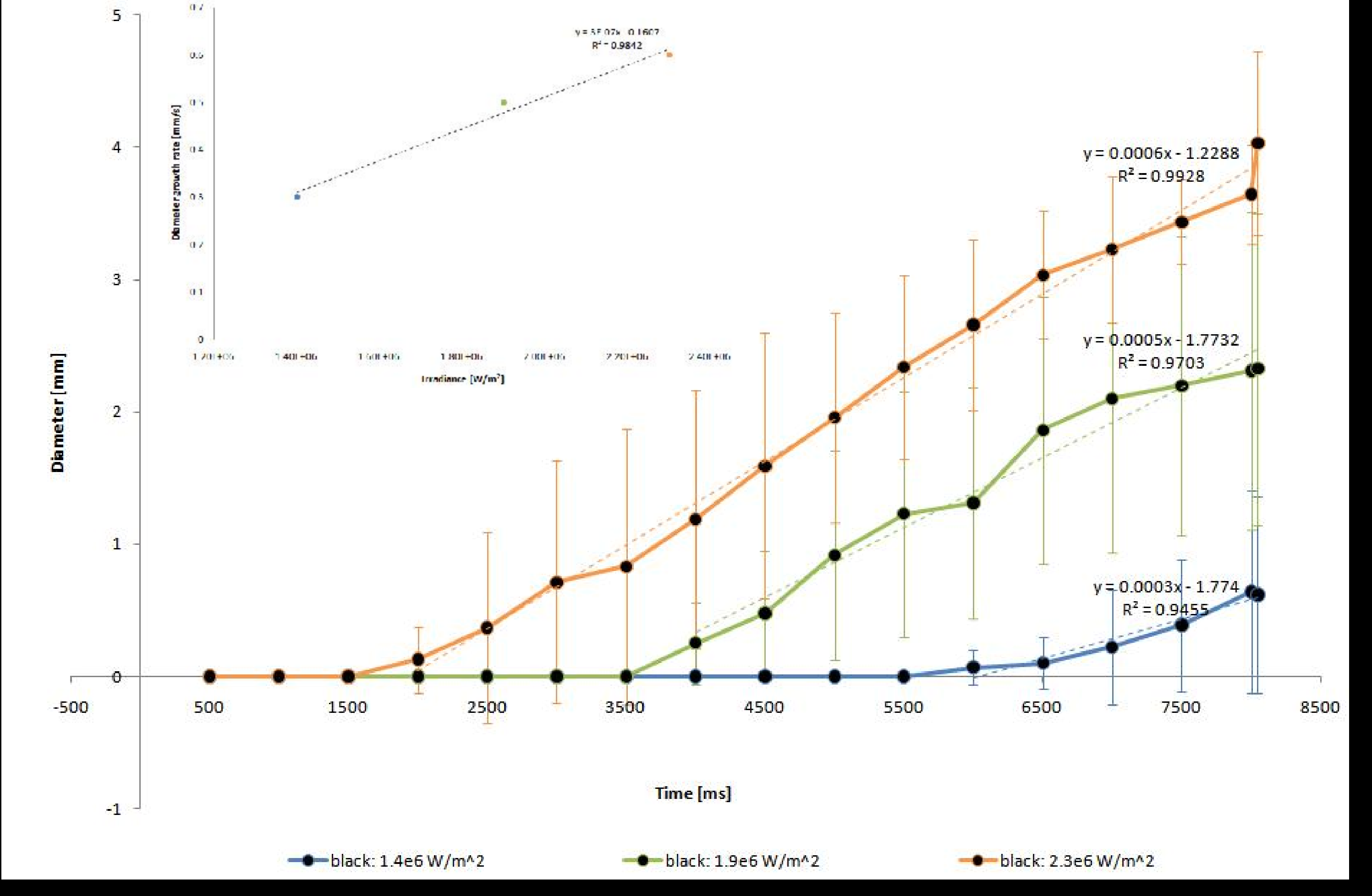

Linear regression of the "black" region growth over time at three irradiances.
Error bars represent 95% CI.

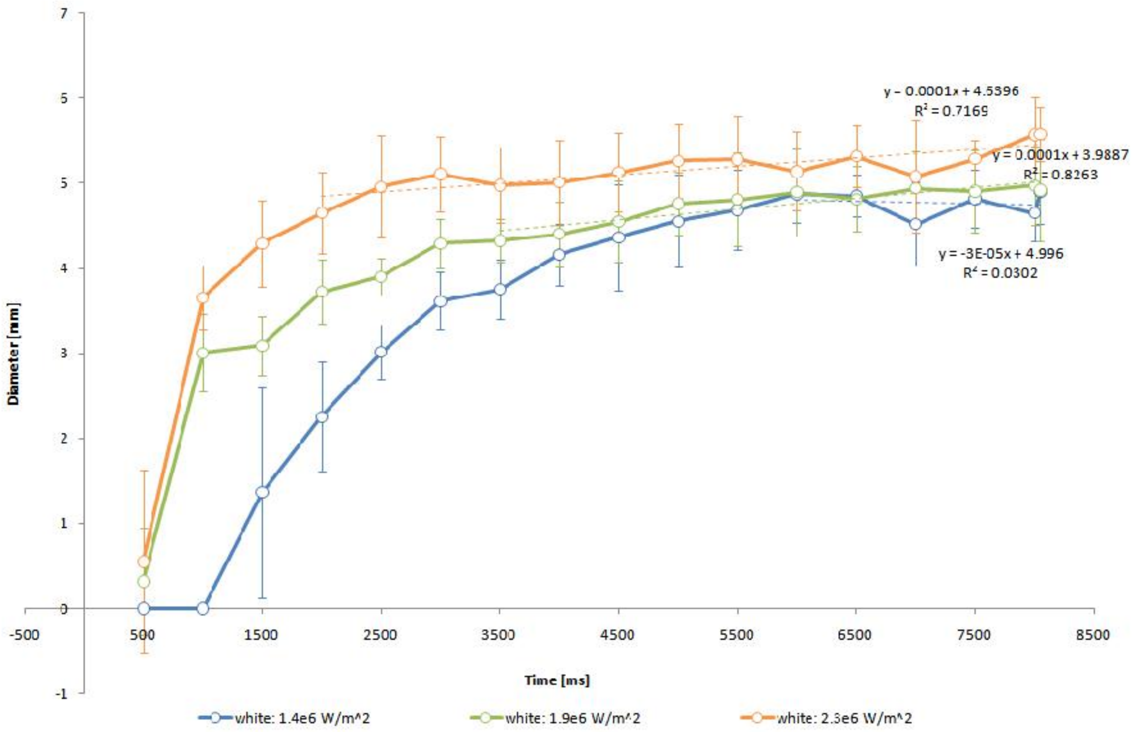

The growth of the "white" region over time at three irradiances. Error bars represent 95% CI.

Average thickness of the coagulated region at three irradiances over time. Error bars represent 95% CI.

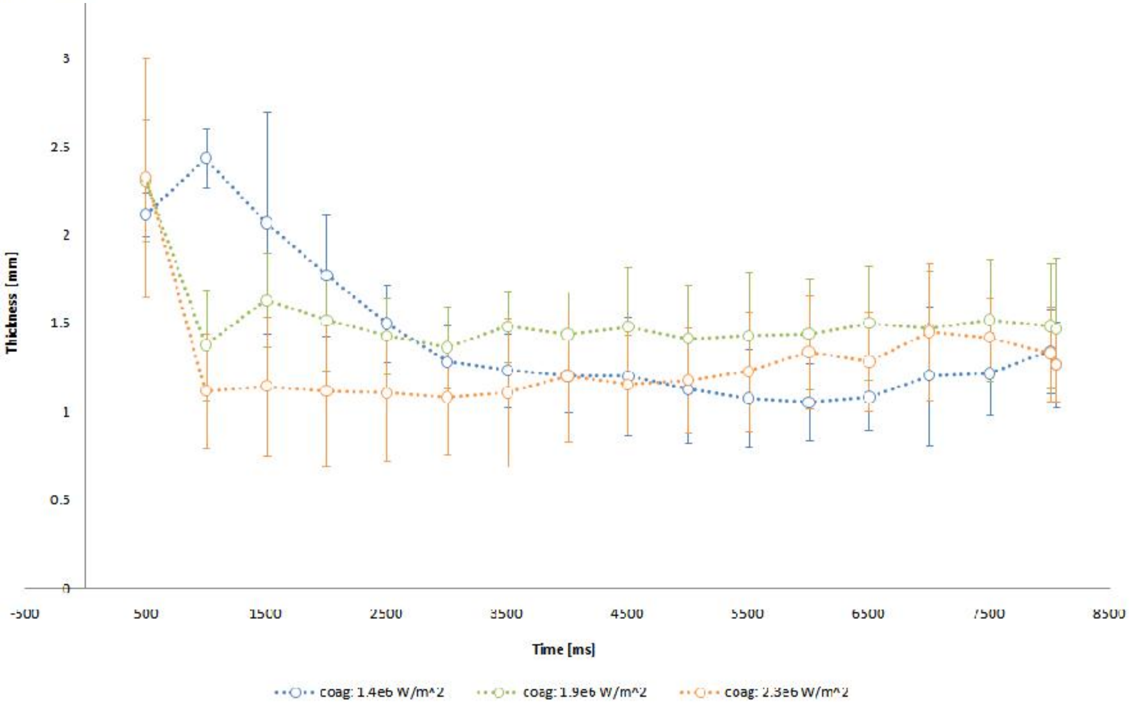

Ablation crater: cross-section video

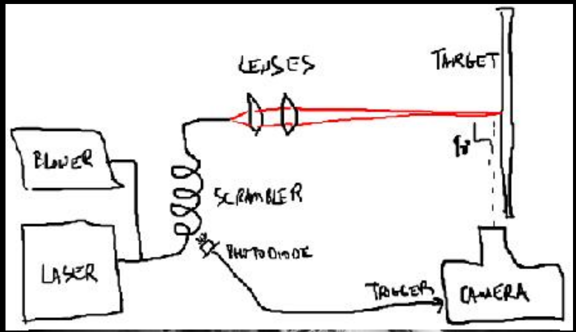

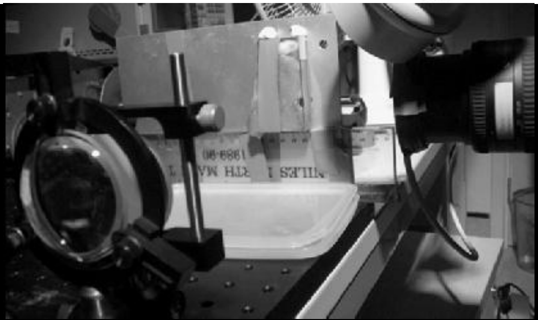

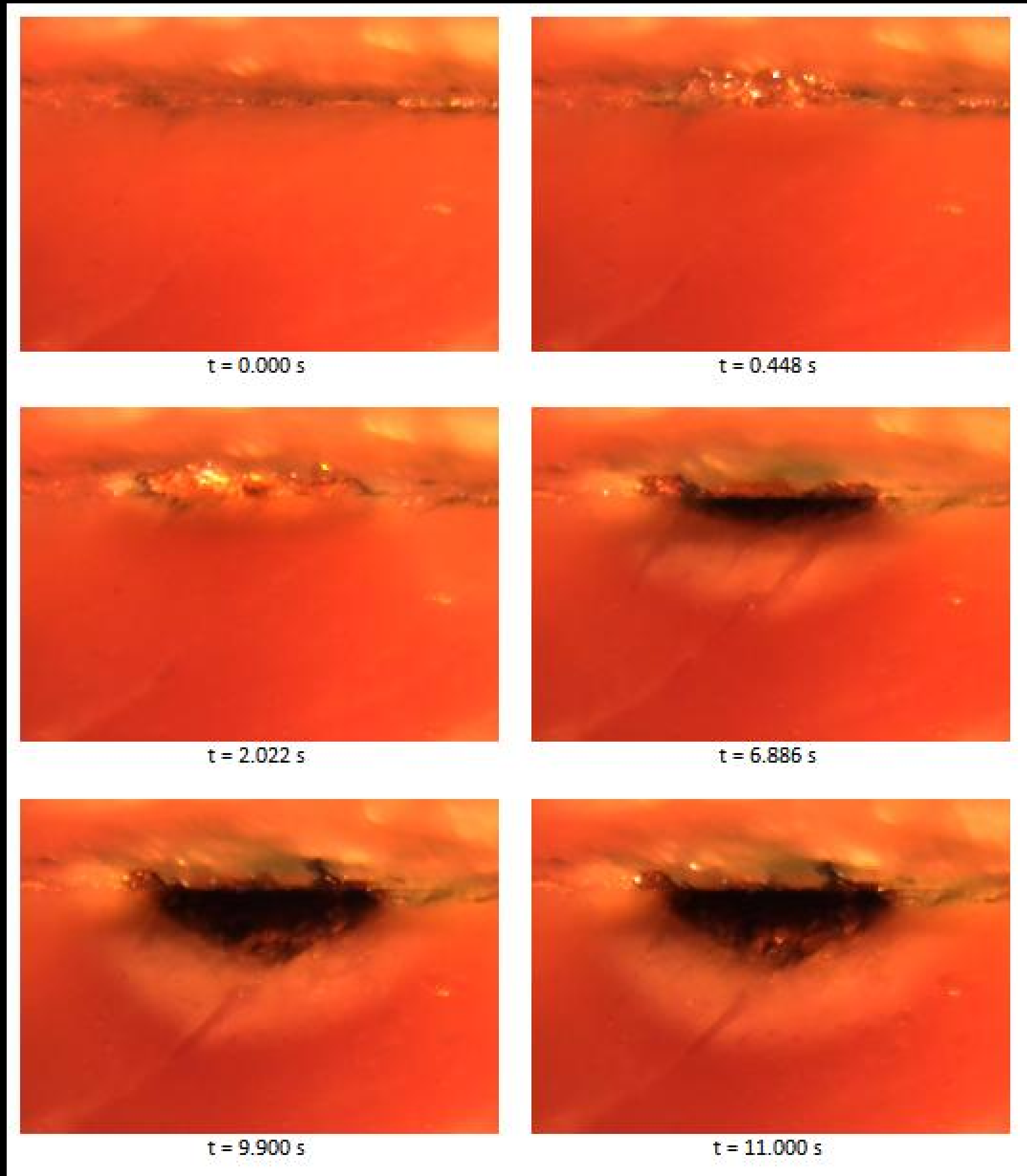

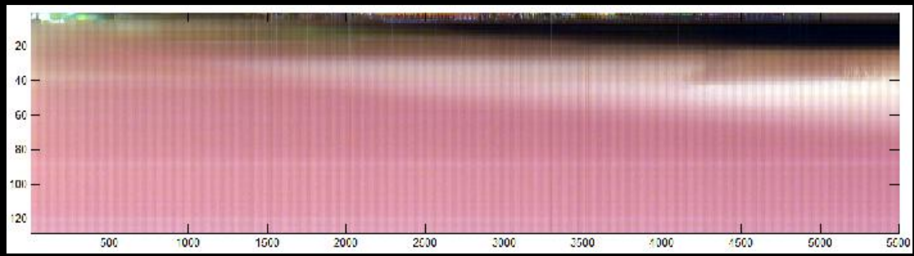

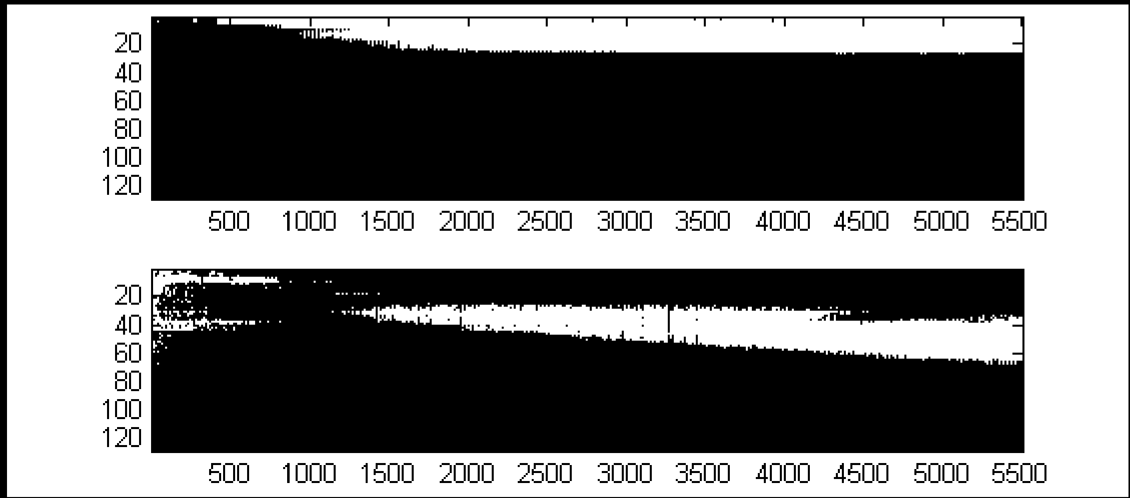

Computer segmentation of regions of black corresponding to the ablation crater and carbonisation (top) and regions of white corresponding to coagulation (bottom).

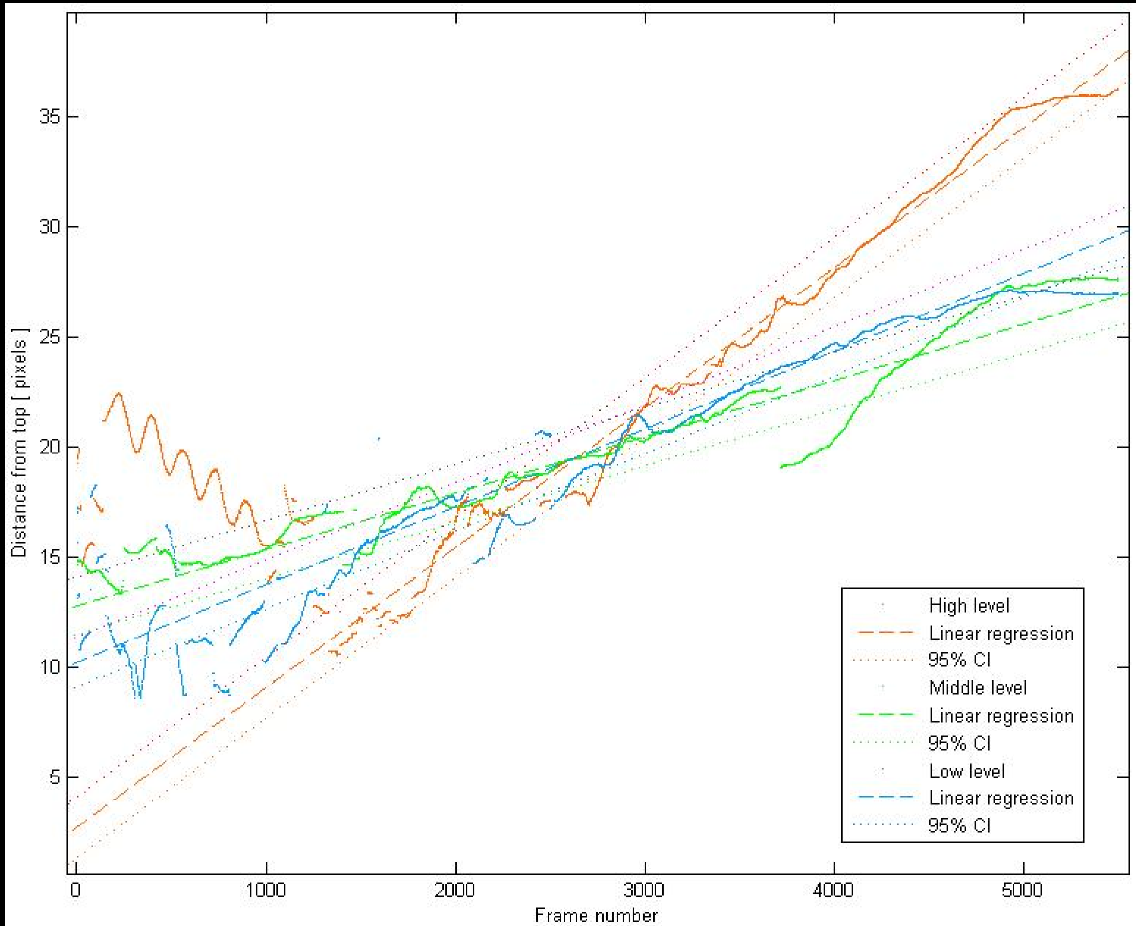

Linear regression of average distance from top of image to the bottom of black region.

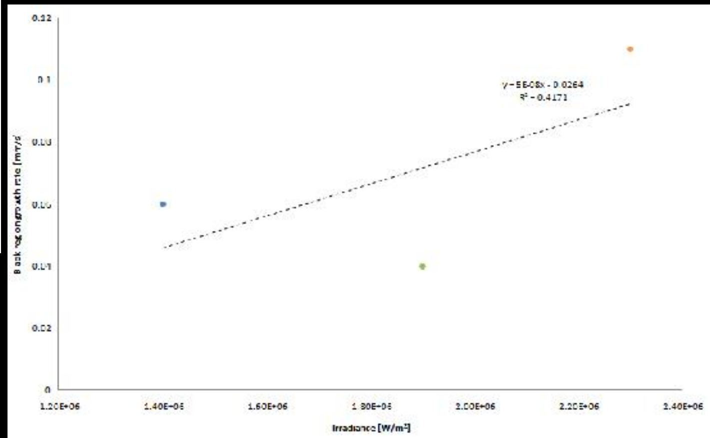

Irradiance	1.4e6 W/m²	1.9e6 W/m²	2.3e6 W/m²
Black region growth rate	0.003524 px/frame (95% CI: ±0.000020)	0.002554 px/frame (95% CI: ±0.000020)	0.006342 px/frame (95% CI: ±0.000030)
y-axis: 29.1 px/mm x-axis: 500 frames/s	0.06 mm/s	0.04 mm/s	0.11 mm/s

Positive correlation between the growth rate of the black region and the irradiance.

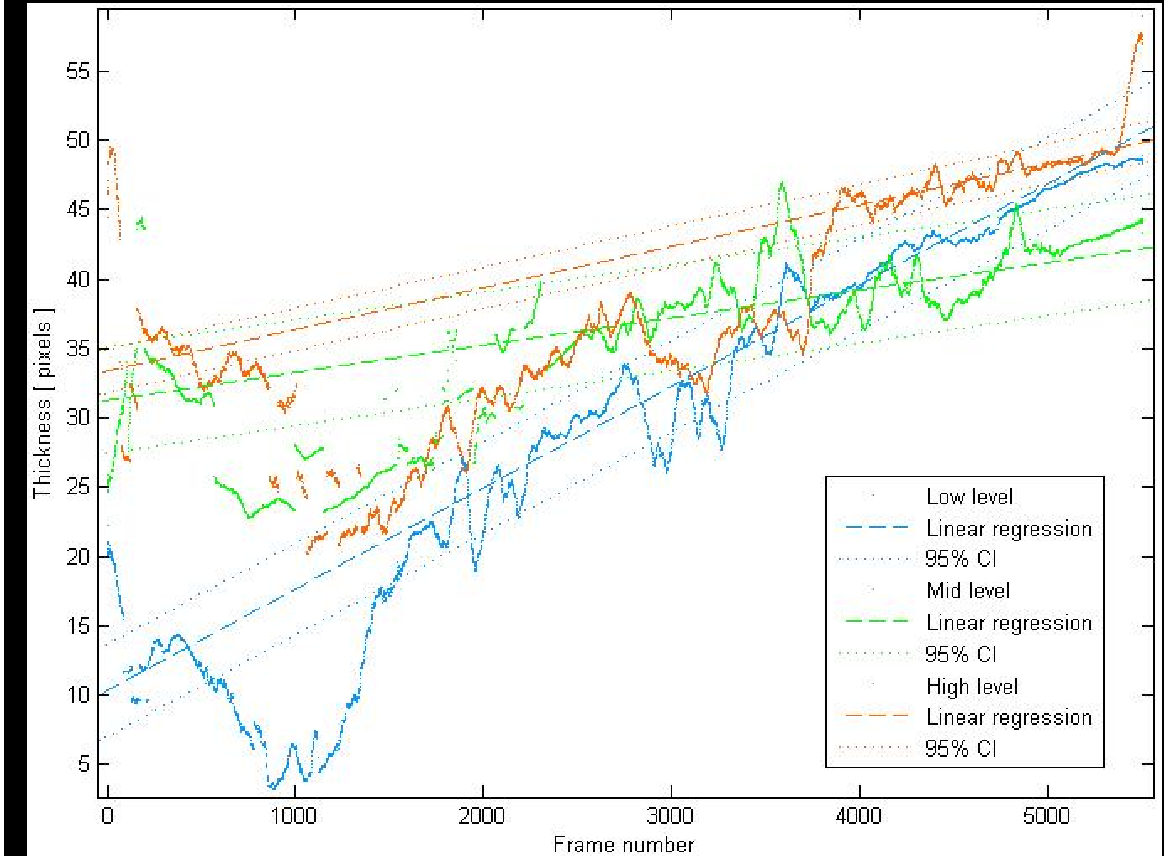

Linear regression of the thickness of the white region.

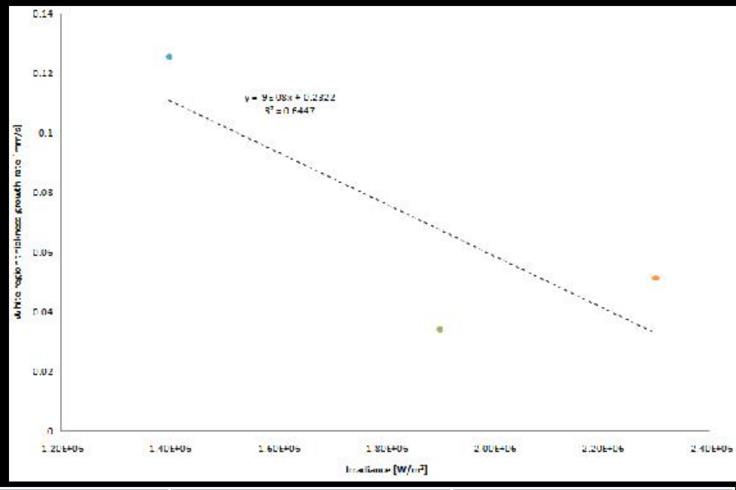

Negative correlation between the growth rate of the thickness of the white region and irradiance.

Irradiance	1.4e6 W/m²	1.9e6 W/m²	2.3e6 W/m²
White thickness growth rate	0.007319 px/frame (95% CI: ±0.000061)	0.001988 px/frame (95% CI: ±0.000100)	0.002997 px/frame (95% CI: ±0.000134)
y-axis: 29.1 px/mm x-axis: 500 frames/s	0.13 mm/s	0.03 mm/s	0.05 mm/s

Statistical model (RSM)

Levels	Irradiance	Exposure time	Dye volume
Low	1.4e6 W/m²	1 s	1 µl
Mid	1.9e6 W/m²	5 s	3 µl
High	2.3e6 W/m²	9 s	5 µl

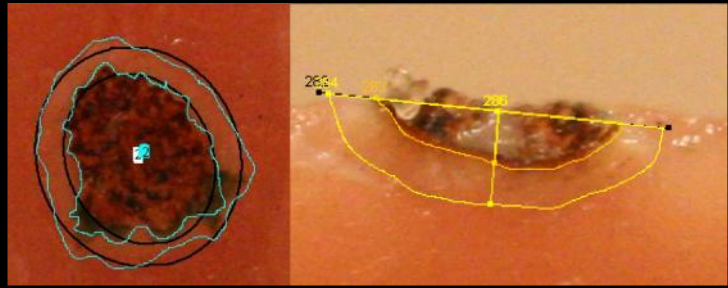

Thickness of the white ROI (en face)

S = 0.145563 PRESS = 0.617807

R-Sq = 42.40% R-Sq(pred) = 30.03%

R-Sq(adj) = 35.21%

Estimated Regression Coefficients for EF-W-thick using data in uncoded units

Term	Coef
Constant	0.289256
Power	0.00274219
Time	0.0371504
Dye	0.0292643

Diameter of the black ROI (en face)

S = 0.514188 PRESS = 10.7108

R-Sq = 66.85% R-Sq(pred) = 41.62%

R-Sq(adj) = 58.21%

Estimated Regression Coefficients for EF-B-dia using data in uncoded units

Term	Coef
Constant	-0.687691
Power	0.208987
Time	0.553146
Dye	0.284268
Power*Power	-0.00504995
Time*Time	-0.0383951
Dye*Dye	-0.0173219

Thickness of the white ROI (cross-section)

S = 0.244147 PRESS = 2.06137

R-Sq = 54.85% R-Sq(pred) = 37.54%

R-Sq(adj) = 49.43%

Estimated Regression Coefficients for X-W-lg using data in uncoded units

Term	Coef
Constant	0.626722
Power	0.0111633
Time	0.0844521
Dye	0.0161031

Depth of the black ROI (cross-section)

S = 0.179180 PRESS = 1.26958

R-Sq = 49.28% R-Sq(pred) = 12.79%

R-Sq(adj) = 36.04%

Estimated Regression Coefficients for X-B-lg using data in uncoded units

Term	Coef
Constant	0.563564
Power	-0.0223531
Time	-0.0580469
Dye	0.162292
Power*Power	0.000778750
Time*Time	0.00970781
Dye*Dye	-0.0280016

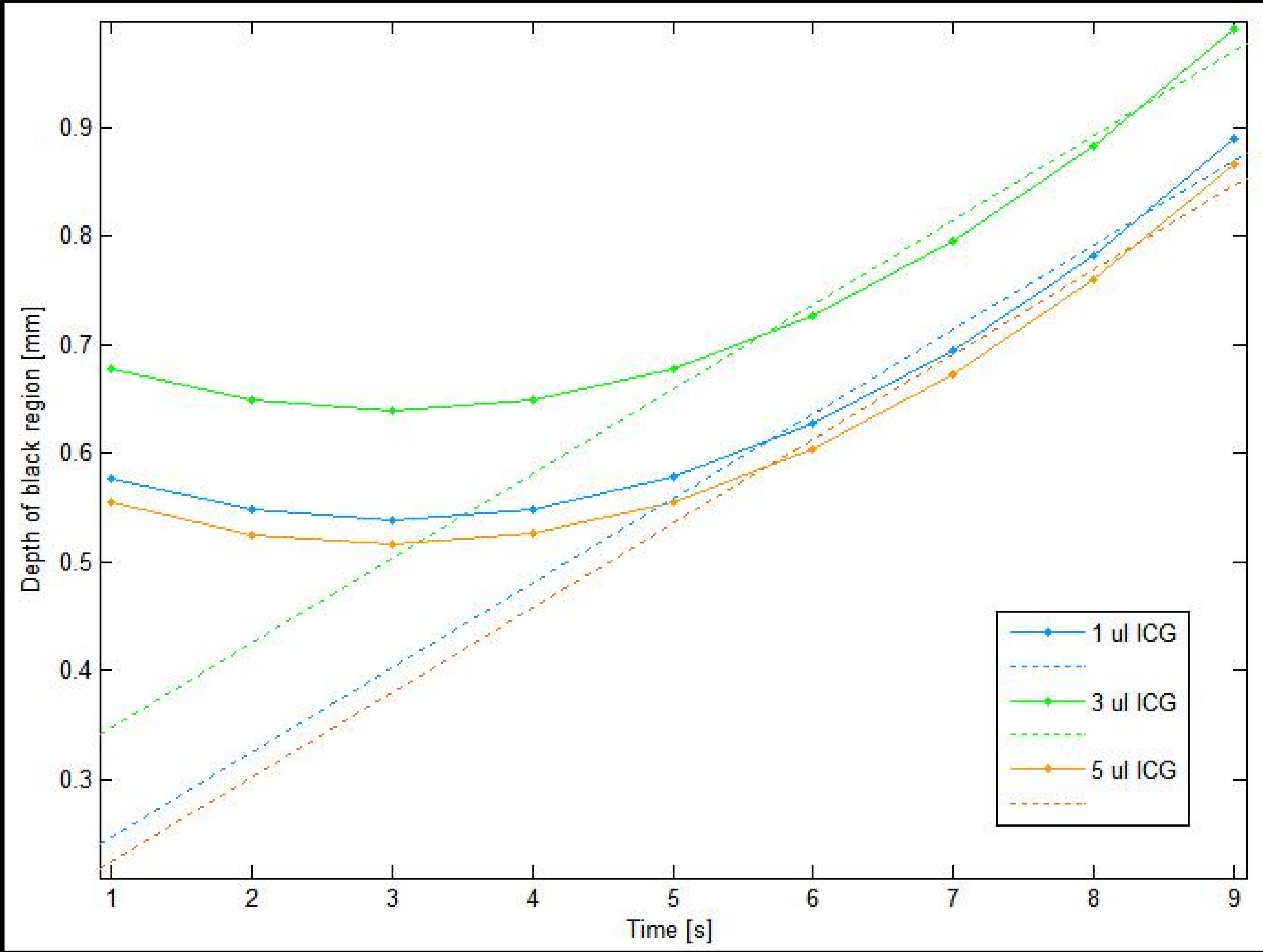

Growth of the black region depth at the high power setting.

Modifications to the standard model

- Dye-mediated laser ablation appears **similar** to normal laser ablation, but there are **differences** too
- Onset & continuation of ICG-mediated ablation – **three phases** similar to Verdaasdonk et al. — (1) ICG-mediated coagulation, (2) ICG-mediated dessication and vaporisation, and (3) cyclic carbonisation
- An **Arrhenius-based model** can be used to model cyclic carbonisation.

Timeline of ICG-mediated ablation

- ICG absorbs 805 nm laser strongly. Heats to **100° C** and water start to boil. Coagulation of underlying tissue by heat conduction.
- Dye solution boils away revealing underlying coagulated tissue.
- ICG can remain intact up to **180° C – 220° C** (Engel et al. 2008)
- Thermal clamp removed – ICG seeds areas of carbonisation. Eventually ICG is displaced or destroyed.
- Char from carbonisation replaces ICG as main absorber. Cyclic carbonisation.
- Solid tissue mass loss further lost by pyrolysis at T > **200° C**, releasing volatiles, water vapour and soot particulates, leaving char behind. In coal, accounts for up to 70% weight loss, but not well known for tissue.
- Superficial layers reach **500° C** and carbon / oxygen combustion dominates, vaporising char into CO.
- In presence of water vapour, gasification of char also can occur, releasing H_2 CO and CO_2. Elevated temperatures above **700° C** required, so probably pyrolysis.
- Potentially vaporisation of carbon at **3350° C**, but not necessary to explain loss of tissue mass.

Multiphysics FEM model

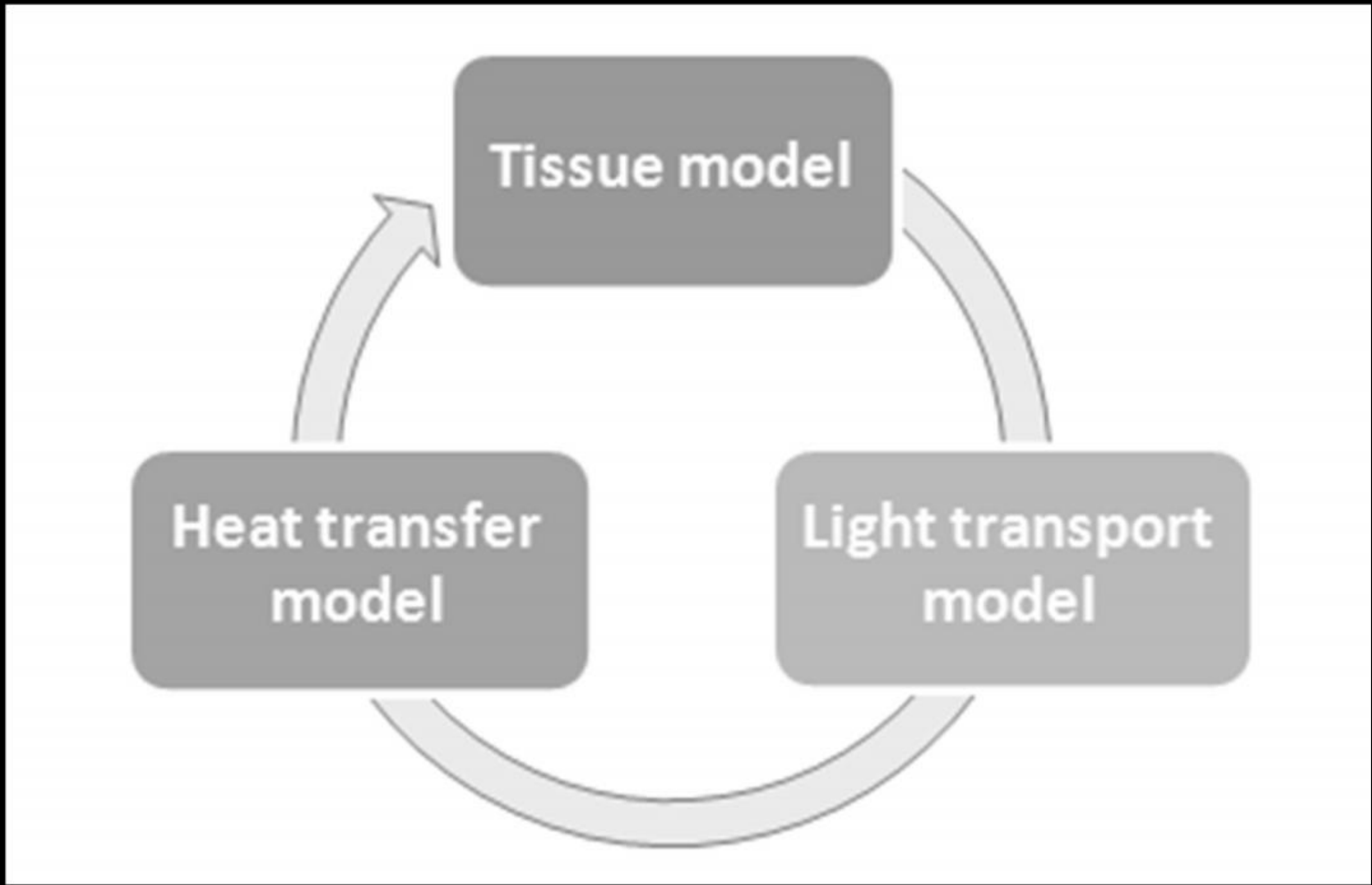

Light transport model

Lambert-Bouguer Law

$$-\frac{dI}{I} = \mu_a \delta l$$

$$I = I_0 e^{-\mu_a y}$$

Heat diffusion model

Penne's Bioheat Equation

$$\rho C \frac{\partial T}{\partial t} + \nabla \cdot (-k \nabla T) = \rho_b C_b \omega_b (T_b - T) + Q_{met} + Q_{ext}$$

Tissue model

Coagulatiion

$$\Omega = \ln\left(\frac{c_x(0)}{c_x(t)}\right) = \int_0^t A e^{\left(-\frac{\Delta E}{RT}\right)} dt'$$

$$F_{uncoagulated} = \frac{c_x(t)}{c_x(0)} = e^{-\Omega}$$

$$\mu_a = F_{uncoagulated}\, \mu_a^{uncoagulated} + F_{coagulated}\, \mu_a^{coagulated}$$

$$F_{uncoagulated} + F_{coagulated} = 1$$

Dessication

$$D = \frac{1}{\sqrt{\pi\, \mathrm{dT}^2}} \exp\left(-\frac{(T - T_{boil})^2}{dT^2}\right)$$

$$C_p^{enthalpy} = DL$$

$$C_p^{step} = (1 - H_{dessication}) C_p^{liquid} + H_{dessication} C_p^{gas}$$

$$C_p = C_p^{step} + C_p^{enthalpy}$$

$$k = (1 - H_{dessication}) k^{liquid} + H_{dessication} k^{gas}$$

$$\rho = (1 - H_{dessication}) \rho^{liquid} + H_{dessication} \rho^{gas}$$

Carbonisation

$$F_{uncarbonised} = \frac{c_x(t)}{c_x(0)} = e^{-\Omega}$$

$$coeff_i = F_{unccarbonised}\, coeff_i^{uncarbonised} + F_{carbonised}\, coeff_i^{carbonised}$$

$$F_{uncarbonised} + F_{carbonised} = 1$$

Vapourisation

$$coeff_i = (1 - H_{vapourisation})\, coeff_i^{unvapourised} + H_{vapourisation}\, coeff_i^{vapourised}$$

THERMAL	Undamaged (C1)	Desiccated @ 100° C (C2)	Carbonised (C3)	Vaporised @ 500° C
Specific heat, Cp [J/(kg K)]	3448 avg. pig skeletal muscle (Duck [276])	1696 pig skin (Knox et al. [333])	1390 char (Shen et al. [321])	2135 steam (NIST)
Thermal conductivity, k [W/(m K)]	0.49 avg. pig skeletal muscle (Duck [276])	0.084 biological fluids (Spells [335])	0.105 char (Shen et al. [321])	0.07 steam (NIST)
Density, ρ [kg/m³]	1041 human skeletal muscle (Duck [276])	270 25.9% not water (Duck [276])	25 10% of charcoal (McKenzie [306])	0.3 steam (NIST)

OPTICAL	Undamaged (C1)	Coagulated (C2)	Carbonised (C3)	Vaporised @ 500° C
Absorption, μ_a [1/cm]	0.30 @ 800 nm pig skeletal muscle (Birth et al. [335])	0.63 (best guess) rat prostate (Skinner et al. [322])	1380 @ 800 nm 10% compact soot (Koylu, Faeth [336])	0.0195 @ 806 nm steam (OMLC)
ICG absorption, μ_a [1/cm]	854 @ 805 nm (measured)	854 @ 805 nm (measured)	1380 @ 800 nm 10% compact soot (Koylu, Faeth [336])	0.0195 @ 806 nm steam (OMLC)

State transition			Model
undamaged	→	coagulated	Arrhenius damage integral drives property changes.
coagulated	→	desiccated	Smooth Heaviside function for property changes. Impulse increase in heat capacity at 100° C for vaporisation.
desiccated	→	carbonised	Arrhenius integral for carbonisation drives property changes.
carbonised	→	vaporised	Smooth Heaviside function for property changes. Impulse decrease in heat capacity at 500° C from combustion.

Results

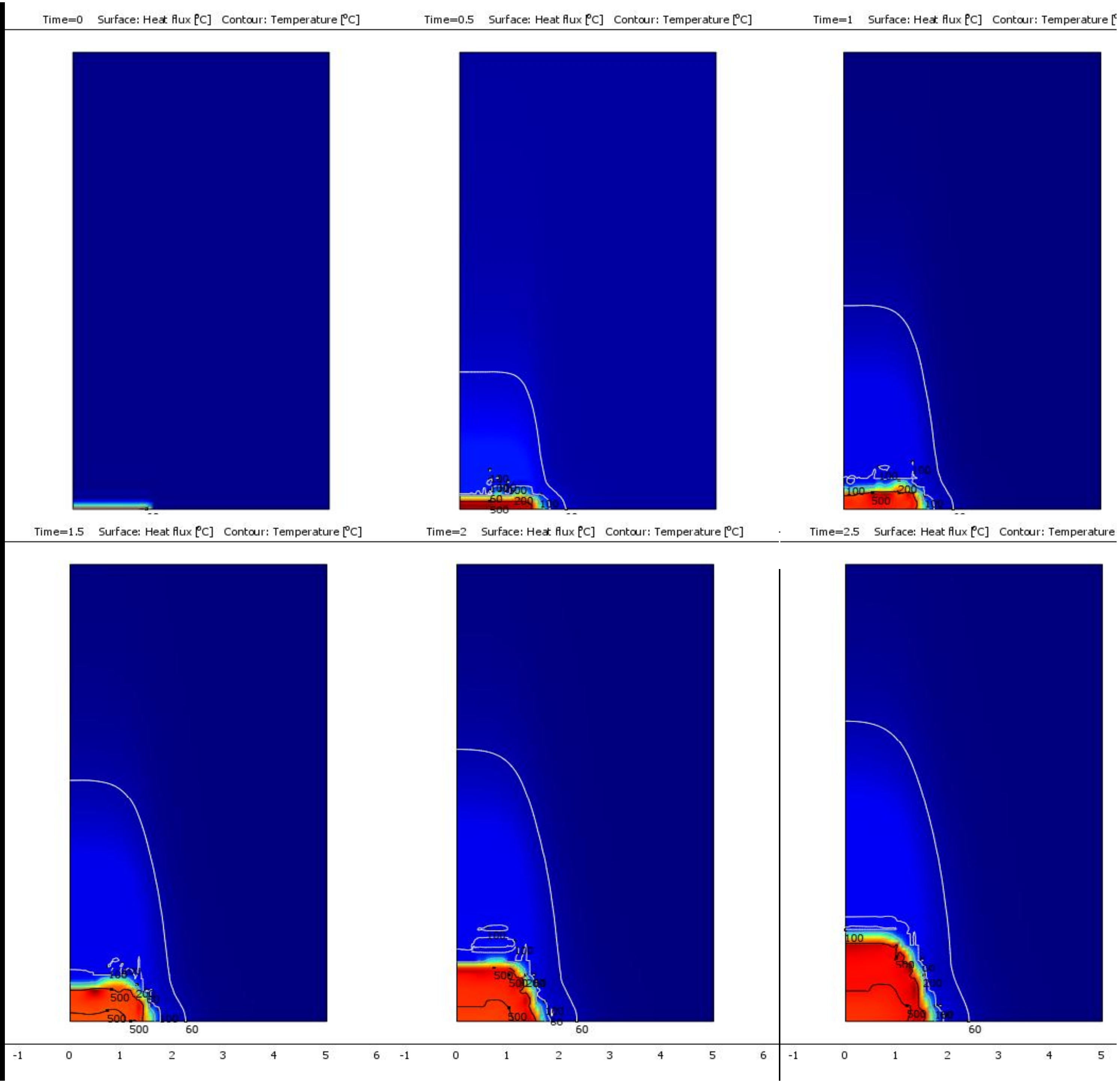

Time=0 Surface: Heat flux [°C] Contour: Temperature [°C]
Time=0.5 Surface: Heat flux [°C] Contour: Temperature [°C]
Time=1 Surface: Heat flux [°C] Contour: Temperature [
Time=1.5 Surface: Heat flux [°C] Contour: Temperature [°C]
Time=2 Surface: Heat flux [°C] Contour: Temperature [°C]
Time=2.5 Surface: Heat flux [°C] Contour: Temperature
500
60
-1 0 1 2 3 4 5 6

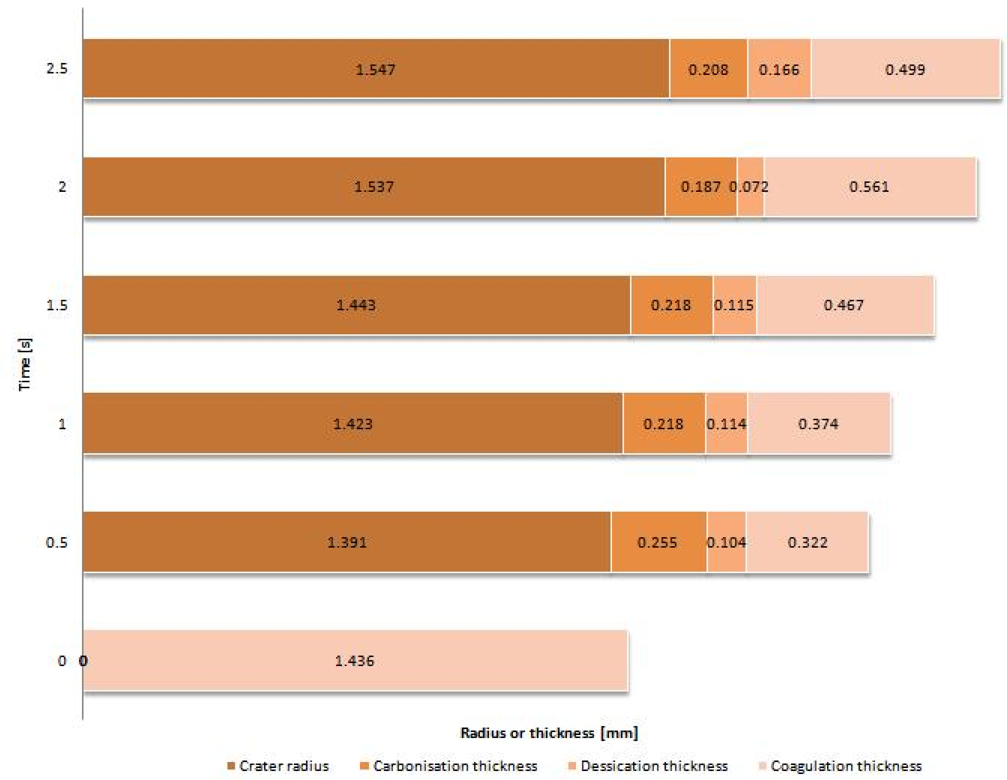

The ablation rate from the computer model is about 0.95 mm/s, which is about twelve times greater than the rate obtained from the RSM model — 0.08 mm/s.

Considering the half slab ablation experiments with the high speed camera in which the ablation rate was 0.11 mm/s, probably half of the thermal energy was lost through the glass plate.

With the full slab, the ablation rate potentially could have been twice as fast, which would make the overestimation of the ablation speed by the computer model to be only a factor of four.

is entirely possible that wood carbonises slower than animal tissues

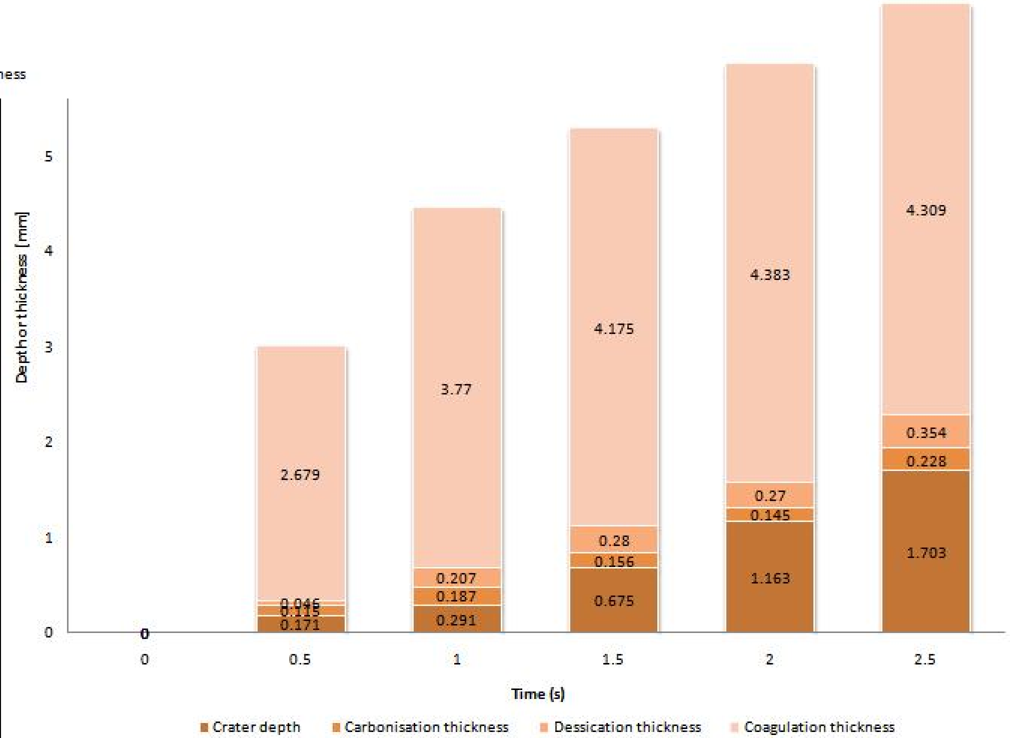

Improvements

Absorption (top), irradiance (middle) and the spatial heat source (bottom) one second into the ablation simulation after replacing the frequency factor in the Arrhenius equation for carbonisation with a higher coefficient.

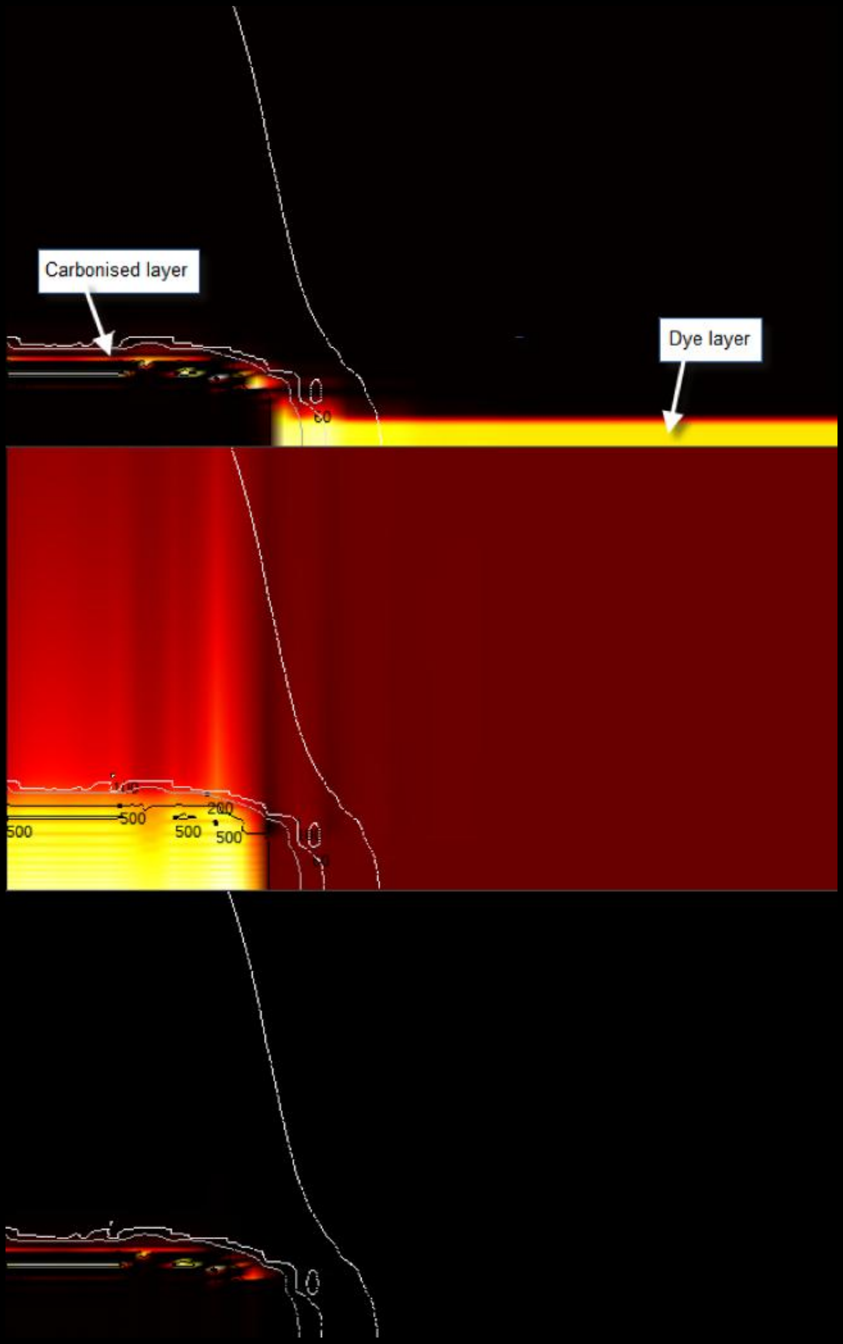

Comparisons to existing methods

Modality	Depth of coagulation necrosis	Source
Scalpel	< 0.01 mm	Molgat et al. [323]
Ultrasonic knife	0.05 mm	von Blomberg et al. [324]
CO_2 laser (ideal)	0.07 mm	Molgat et al. [323]
Ultrasonic knife	0.30 – 0.38 mm	Morosolli et al. [325]
Monopolar electrosurgery	0.30 – 0.38 mm	Morosolli et al. [325]
CO_2 laser	0.30 – 0.38 mm	Morosolli et al. [325]
Monopolar electrosurgery	0.35 mm	von Blomberg et al. [324]
Hot scalpel	0.34 mm	Molgat et al. [323]
Bipolar electrosurgery	1 mm	Botto et al. [242]
Monopolar electrosurgery	1.01 mm	Molgat et al. [323]
CO_2 laser	1.88 mm	Molgat et al. [323]
Ho:YAG laser	3-4 mm	Botto et al. [242]

From the statistical model, at 25 W set power and 5 µl ICG, dye mediated laser ablation would cause a coagulation depth beneath the ablation crater of 1.07 – 1.75 mm with exposure times of 1 – 9 s. This is comparable to reported damage caused by electrosurgery and ablation by other types of lasers.

Potential dye application methods

- Droplets and marker pens
- Injections and tattoos
- Chalk-lines and stitches
- Stamps and stencils

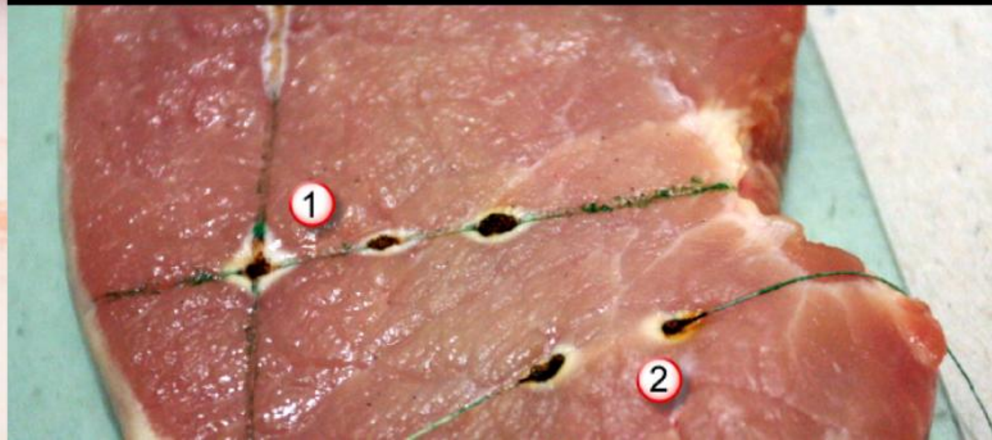

Potential methods for erasure

- Waterjet cleaning
- Photobleaching ICG
- Methylene blue and its leuco form

Conclusions:

1. Why? — **Why** should we do it?
   New tools are needed.
2. What? — **What** should we do?
   White space does exist. DD.
3. How? — **How** do we do it?
   DD concepts were explored.
4. How? — **How** do we **really** do it?
   Dye-mediated ablation is possible. Foundation set.